Atmos. Chem. Phys., 22, 13467–13493, 2022
https://doi.org/10.5194/acp-22-13467-2022

Atmospheric Chemistry and Physics
Open Access
EGU

Significant formation of sulfate aerosols contributed by the heterogeneous drivers of dust surface

Tao Wang[1], Yangyang Liu[1], Hanyun Cheng[1], Zhenzhen Wang[1], Hongbo Fu[1], Jianmin Chen[1], and Liwu Zhang[1,2]

[1]Shanghai Key Laboratory of Atmospheric Particle Pollution and Prevention, National Observations and Research Station for Wetland Ecosystems of the Yangtze Estuary, IRDR international Center of Excellence on Risk Interconnectivity and Governance on Weather, Department of Environmental Science & Engineering, Fudan University, Shanghai, 200433, Peoples' Republic of China
[2]Shanghai Institute of Pollution Control and Ecological Security, Shanghai, 200092, Peoples' Republic of China

Correspondence: Liwu Zhang (zhanglw@fudan.edu.cn)

Received: 23 March 2022 – Discussion started: 22 April 2022
Revised: 14 September 2022 – Accepted: 25 September 2022 – Published: 19 October 2022

Abstract. The importance of dust heterogeneous oxidation in the removal of atmospheric SO_2 and formation of sulfate aerosols is not adequately understood. In this study, the Fe-, Ti-, and Al-bearing components, Na^+, Cl^-, K^+, and Ca^{2+} of the dust surface, were discovered to be closely associated with the heterogeneous formation of sulfate. Regression models were then developed to make a reliable prediction of the heterogeneous reactivity based on the particle chemical compositions. Further, the recognized gas-phase, aqueous-phase, and heterogeneous oxidation routes were quantitatively assessed and kinetically compared by combining the laboratory work with a modelling study. In the presence of 55 $\mu g\,m^{-3}$ airborne dust, heterogeneous oxidation accounts for approximately 28.6 % of the secondary sulfate aerosols during nighttime, while the proportion decreases to 13.1 % in the presence of solar irradiation. On the dust surface, heterogeneous drivers (e.g. transition metal constituents, water-soluble ions) are more efficient than surface-adsorbed oxidants (e.g. H_2O_2, NO_2, O_3) in the conversion of SO_2, particularly during nighttime. Dust heterogeneous oxidation offers an opportunity to explain the missing sulfate source during severe haze pollution events, and its contribution proportion in the complex atmospheric environments could be even higher than the current calculation results. Overall, the dust surface drivers are responsible for the significant formation of sulfate aerosols and have profound impacts on the atmospheric sulfur cycling.

1 Introduction

As an important component of atmospheric particulate matter, sulfate exerts profound impacts on the Earth's climate system, air quality, and public health (Seinfeld and Pandis, 2016; W. Wang et al., 2021). The rapid formation of sulfate was proven to be largely responsible for London fog and Beijing haze (G. Wang et al., 2016; Cheng et al., 2016). Secondary sulfate aerosols originate predominately from the conversion of sulfur dioxide (SO_2) via the gas-phase oxidation in gaseous environments, aqueous-phase oxidation in liquid media, and heterogeneous oxidation on aerosol surfaces (Ravishankara, 1997; Mauldin III et al., 2012; Su et al., 2020; T. Liu et al., 2021). In recent years, the newly found sulfate formation pathways were kinetically compared with the documented ones to evaluate the relative importance of them (Cheng et al., 2016; Gen et al., 2019; T. Liu et al., 2020; X. Wang et al., 2020). In addition, the reported oxidation channels were compared with each other by aerosol observations or modelling investigations (Berglen et al., 2004; Sarwar et al., 2013; He et al., 2018; Ye et al., 2018; Fan et al., 2020; Tao et al., 2020; Zheng et al., 2020; Song et al., 2021;

Tilgner et al., 2021; Y. Liu et al., 2021; Gao et al., 2022; S. Wang et al., 2022; Ye et al., 2022). In general, these studies emphasized the importance of certain newly discovered aqueous-phase processes or compared the contributions from the documented gas- and aqueous-phase pathways. Nevertheless, heterogeneous reaction was scarcely involved in the discussion, thus hindering the deeper understanding of the atmospheric relevance of aerosol surfaces.

Heterogeneous reaction alters the concentrations of gas-phase SO_2 and particle-phase sulfate, and its atmospheric influences were considered by observation and modelling works (Fairlie et al., 2010; Alexander et al., 2012; Chen et al., 2017; K. Wang et al., 2021). As summarized by Table S1, when simulating the sulfate burst events, researchers observed the positive feedbacks after implementing a heterogeneous mechanism in the WRF-Chem (G. Li et al., 2017), GEOS-Chem (Shao et al., 2019), CAMx (Huang et al., 2019), and CMAQ (S. Zhang et al., 2019) models. However, these improved models highlighted the heterogeneous oxidation motivated by the surface-adsorbed oxidants rather than the heterogeneous drivers of aerosol surfaces. To address the knowledge gap, the revised GEOS-Chem (Y. Wang et al., 2014) and WRF-CMAQ (Zheng et al., 2015) models considered the heterogeneous oxidation driven by aerosol surfaces and successfully reproduced the rapid sulfate formation. Xue et al. (2016) moved forward to develop an observation-based model and found that a heterogeneous pathway contributed up to one-third of the secondary sulfate in a typical haze–fog event. However, the "aerosol surface" mentioned in the previous works was not distinguished by its physical or chemical properties (Y. Wang et al., 2014; Zheng et al., 2015; Xue et al., 2016), thereby making it difficult to compare the atmospheric importance of the diverse airborne surfaces. As discussed above, it is of great importance to investigate the heterogeneous drivers of one selected aerosol surface and further evaluate the atmospheric significance of the relevant heterogeneous pathway.

The resurgence of sandstorms in North China makes the air pollution situation more complex than ever before. The concentration of PM_{10} (particulate matter with an aerodynamic diameter of less than 10 µm) in Beijing reached up to 3600 µg m^{-3}, largely beyond the standards of the World Health Organization and the Chinese government (G. Li et al., 2021). As the most abundant primary aerosol in the troposphere (Textor et al., 2006; Tang et al., 2016), dust particles could transport more than one full circuit around the globe within ∼ 2 weeks (Uno et al., 2009) and concurrently participate in an array of atmospheric reactions. Heterogeneous reactions over the dust surface consume and produce various trace gases, thereby affecting the dust property and tropospheric oxidation capacity (Tang et al., 2016). One of the most extensive concerns is that the numerous surface sites of wind-blown dust provide opportunities for a variety of atmospheric reactions to occur, e.g. oxidation of SO_2 and formation of sulfate (Usher et al., 2003). In the past decades, plenty of laboratory works have been performed to explore the heterogeneous behaviours of SO_2 on dust surfaces.

When discussing the heterogeneous oxidation on a dust proxy, environmental factors like humidity, temperature, and irradiance were frequently concerned. Adsorbed water not only helps to accumulate surface $S_{(IV)}$ species, but also competes with SO_2 for surface sites (Rubasinghege and Grassian, 2013). The reversible adsorption of SO_2 is believed to be exothermic (Clegg and Abbatt, 2001a). In contrast, there were positive temperature dependences observed for $CaCO_3$ below 250 K over the entire reaction (Wu et al., 2011) and for Fe_2O_3 within 284–318 K during the initial reaction stage (T. Wang et al., 2018a). Light irradiation normally accelerates the transformation of (bi)sulfites to (bi)sulfates (J. Li et al., 2010; Nanayakkara et al., 2012; Han et al., 2021), while iron oxides may undergo photo-reactive dissolution and thus exhibit weaker reactivity under sunlight (Fu et al., 2009). The reactivity can be enhanced by H_2O_2 (Huang et al., 2016), O_3 (L. Li et al., 2006, 2007; Y. Zhang et al., 2018), NO_x (Ma et al., 2008; C. Liu et al., 2012; He et al., 2014; Yu et al., 2018; Zhao et al., 2018; W. Yang et al., 2018a; H. Wang et al., 2020), NH_3 (W. Yang et al., 2016, 2018b, 2019), or Cl_2 (Huang et al., 2017). By contrast, organic compounds, like CH_3CHO (Zhao et al., 2015), HCOOH (Wu et al., 2013), CH_3COOH (N. Yang et al., 2020; R. Wang et al., 2022), and C_3H_6 (Chu et al., 2019), were found to suppress the interactions due to the accumulation or production of particle-phase organic acids. Moreover, CO_2 hinders the heterogeneous oxidation under dark conditions (Y. Liu et al., 2020) but presents positive impacts on sulfate formation under solar irradiation (Y. Liu et al., 2022). The particle physical properties, including size (Baltrusaitis et al., 2010; Y. Zhang et al., 2016), morphology (K. Li et al., 2019), and crystal structure (W. Yang et al., 2017), display varied impacts on heterogeneous reaction. When considering the particle chemical properties, Fe_2O_3 is more active than Al_2O_3 and SiO_2 in the heterogeneous uptake of SO_2 and formation of sulfate (Chughtai et al., 1993; X. Zhang et al., 2006; He et al., 2014). Furthermore, the presence of moderate nitrate (Kong et al., 2014; Du et al., 2019), Al_2O_3 (T. Wang et al., 2018b), surfactant (Zhanzakova et al., 2019), oxalate (K. Li et al., 2021), or (bi)carbonate (Y. Liu et al., 2022) on dust surfaces could favour the heterogeneous kinetics under specific conditions. Relative to the environmental factors, the heterogeneous effects relevant to particle properties are still under debate.

The usage of a simple mineral oxide as a substitute for natural dust may be problematic, as such an approach could undermine the atmospheric importance of more complex mineralogy. Authentic dusts were utilized in laboratory works (Table S2). Some studies concerned single samples like Saharan dust (Ullerstam et al., 2002, 2003; Adams et al., 2005; Harris et al., 2012), Arizona test dust (Park and Jang, 2016; S. Zhang et al., 2019; Y. Zhang et al., 2019), Chinese loess (Usher et al., 2002), and Asian dust (Ma et al., 2012). The comparison of diverse samples has been attracting increasing

attention. Zhou et al. (2014) observed the positive temperature effect on Xinjiang sierozem, in contrast to the negative temperature dependence for Inner Mongolian desert dust. Huang et al. (2015) discovered the accelerated oxidation of SO_2 by H_2O_2 and attributed the different moisture effects to the dusts' varying components. Maters et al. (2017) explored the heterogeneous uptake on volcanic ash and glass samples and related the reactivity differences to the varying abundances of surface basic and reducing sites. Park et al. (2017) compared the heterogeneous reactions on Gobi desert dust and Arizona test dust and linked the sulfate formation to the quantity of semi-conductive metals. Z. Wang et al. (2019) discovered the enhanced uptake of SO_2 on clay minerals after the simulated cloud processing and explained this evolution by the modification of iron speciation. Urupina et al. (2019) discussed the kinetics of diverse volcanic dusts and further experimentally proved that neither one selected pristine oxide nor a mixture of them can adequately typify the behaviour of natural dust (Urupina et al., 2021). Recently, based on the measurement method for sulfite and sulfate (Urupina et al., 2020), they determined the associations between sulfate production and dust chemical properties like (Fe + Al) / Si and Na abundance (Urupina et al., 2022). The aforementioned works broaden the horizons of the heterogeneous drivers on the dust surface. Up to now, the dominant dust surface drivers have remained controversial due to the limited statistical linkages between the chemical composition of dust and the production rate of sulfate.

While the atmospheric relevance of the oxidation of SO_2 on dust has been widely recognized (Wu et al., 2020; Xu et al., 2020), the contribution of dust heterogeneous oxidation to secondary sulfate aerosols has not been quantitatively determined. By means of the improved WRF-CMAQ model, K. Wang et al. (2012) attributed a 27 % decrement of SO_2 concentration and a 12 % increment of sulfate concentration to the heterogeneous processes during an Asian dust storm. Moreover, Tian et al. (2021) recently simulated the heterogeneous formation of dust sulfate with the revised GEOS-Chem model and found that, during the dust episodes in North China, up to 30 % of the secondary sulfate resulted from the heterogeneous processes on the dust surface. However, the photocatalytic reactivity of dust was not considered by the advanced models. Yu et al. (2017) developed the atmospheric mineral aerosol reaction (AMAR) model based on the laboratory works and suggested that the heterogeneous photocatalysis of the mineral dust surface contributed more than half of the secondary sulfate. However, the heterogeneous reactivity was measured by quantifying all the adsorbed SO_2 rather than calculating the yield of particle-phase sulfate. Moreover, limited gas- and aqueous-phase pathways were included in these models, and the heterogeneous reactivities of surface-adsorbed oxidants and dust surface drivers have not been distinguished yet. Therefore, it is highly desirable to comprehensively compare the dust heterogeneous pathways with other documented sulfate formation pathways.

Hereby, upon understanding the driving factors and driving force of the airborne dust surface, this work compared dust heterogeneous pathways with the gas- and aqueous-phase ones with respect to the formation rate of sulfate and the atmospheric lifetime of SO_2. In order to characterize the sensitivity of heterogeneous reaction to dust loading, the scenarios with different dust concentrations were also considered. The joint influences of ionic strength and aerosol liquid water content on the aqueous-phase oxidation of SO_2 were further discussed to prove the significance of heterogeneous kinetics under diverse atmospheric conditions. The recently reported microdroplet interfacial oxidations were additionally compared with the dust-related heterogeneous pathways to emphasize the atmospheric relevance of dust surface drivers. This study attempted to verify the significant formation of sulfate aerosols contributed by the heterogeneous drivers of the dust surface.

2 Methods

2.1 Methodology overview

This study attempted to investigate whether the heterogeneous oxidation of SO_2 on the dust surface, particularly that induced by the dust surface drivers, makes great impacts on the loss of gaseous SO_2 and formation of sulfate aerosols (Text S1, Fig. S1). The gas- and aqueous-phase pathways were assessed by the documented methodologies and parameterizations (Cheng et al., 2016; Seinfeld and Pandis, 2016; Shao et al., 2019; Song et al., 2021), as briefly introduced by Sect. 2.2 (more details in the Supplement). The heterogeneous conversion of SO_2 comprises dust-mediated and dust-driven modes, emphasizing the oxidants co-adsorbed with SO_2 and the drivers of the dust surface, respectively. In the dust-mediated mode, the dust surface functions as a reaction medium that supports the interaction between adsorbed oxidants and SO_2. In the dust-driven mode, the oxidation of adsorbed SO_2 is initiated by the active components of the dust surface. The former mode was assessed by the particle properties based on the reported methodology, while the latter mode was quantitatively characterized by the laboratory works.

2.2 Gas- and aqueous-phase oxidation pathways

The gas-phase oxidation of SO_2 is initiated by a hydroxyl radical (OH), stabilized Criegee intermediates (CIs), and a nitrate radical (NO_3). The former two oxidants promote the sulfate formation during daytime, while the latter one works mainly during nighttime. More details can be found in Text S2.

The aqueous-phase sulfate formation is pH-dependent and can be quantified based on the published documents and the references cited therein (Cheng et al., 2016; Su et al., 2020; T. Liu et al., 2021a). Herein, an aqueous-phase pathway

refers to the liquid SO_2 conversion by the transition-metal ion-catalysed oxygen (TMI-O_2), ozone (O_3), hydrogen peroxide (H_2O_2), nitrogen oxide (NO_2), methyl hydroperoxide (CH_3OOH), peroxyacetic acid (CH_3COOOH), hypochlorous acid (HOCl), hypobromous acid (HOBr), dissolved nitrous acid (HONO), photosensitization (T^*), and nitrate photolysis ($P_{NO_3^-}$). The processes relevant to T^* and $P_{NO_3^-}$ are only considered for the daytime scenario. More details can be found in Text S3 and Tables S3–S4.

The oxidant concentration data were derived from the atmospheric observation campaigns performed in Beijing, North China. The measurements conducted in warm seasons were considered in priority to correspond to the experimental temperature. The relevant temperature range is 293–303 K and is representative of the warm season. Considering the relatively high irradiance used in the laboratory experiments, the oxidant parameters for daytime discussion were selected from the observations performed at noontime. The influences of dust loading on the oxidant concentrations, nitrate photolysis kinetics, and TMI abundances were considered to reflect the linkages between different reactions. More details can be found in Text S4 and Table S5.

2.3 Heterogeneous oxidation-particle characterizations

Five airborne clay minerals, including nontronite (NAu), chlorite (CCa), montmorillonite (SWy), kaolinite (KGa), and illite (IMt), were obtained from the Source Clay Minerals Repository (Purdue University, West Lafayette, Indiana, USA). The purchased clays were sent for the following measurements.

The clay minerals were analysed with an X-ray fluorescence spectrometer (Axios Advanced, PANalytical, Netherlands) for element distributions (Table S6). The Brunauer–Emmett–Teller (BET)-specific surface areas (S_{BET}) of NAu, CCa, SWy, KGa, and IMt were measured with a Quantachrome Nova 1200 BET apparatus to be 19.76, 5.67, 22.64, 18.77, and 20.05 $m^2\,g^{-1}$, respectively.

Particles were suspended in Milli-Q water (18.2 MΩ cm at 25°) before the size measurement (ViewSizer™ 3000, MANTA Instruments, USA). The particle diameters range mostly from 50 to 1000 nm and are averaged to 399 nm for NAu, 272 nm for CCa, 438 nm for SWy, 396 nm for KGa, and 366 nm for IMt (Fig. S2).

Prepared particles were ultrasonically extracted in Milli-Q water, followed by the filtration through a polytetrafluoroethylene membrane filter. The obtained solution was analysed by ion chromatography (883 Basic, Metrohm, Switzerland) for the concentrations of anions ($HCOO^-$, Cl^-, NO_3^-, SO_4^{2-}) and cations (Na^+, NH_4^+, K^+, Mg^{2+}, Ca^{2+}) (Fig. S3) by the reported methods (Wang et al., 2020b). The water-soluble ions account for 4.6 ‰, 0.1 ‰, 8.5 ‰, 0.3 ‰, and 0.8 ‰ of the mass contents of NAu, CCa, SWy, KGa, and IMt, respectively.

A mixture, denoted as natural dust hereafter, was prepared by mechanically mixing the studied clay minerals with their atmospheric abundances. Because the clays in the kaolinite group (NAu, KGa), montmorillonite group (SWy), illite group (IMt), and chlorite group (CCa) occupy, respectively, 6.6 %, 4.0 %, 53.8 %, and 4.3 % mass fractions of the airborne dust (Usher et al., 2003), the prepared natural dust sample comprises 8.8 wt % of NAu, 8.8 wt % of KGa, 5.3 wt % of CCa, 71.4 wt % of IMt, and 5.7 wt % of CCa.

2.4 Heterogeneous oxidation–DRIFTS measurements

The in situ DRIFTS (diffuse reflectance infrared Fourier transform spectroscopy) spectra were collected using a FTIR spectrometer (Tracer-100, Shimadzu, Japan) equipped with a mercury–cadmium–telluride detector cooled by liquid nitrogen. A gas supply system was constructed by linking the experimental units through Teflon tubes. Mass flow controllers (D07-19, Severstar, China) adjusted the reactant gases to the expected reactant concentration and relative humidity (RH). Gas cylinders had high-purity air (79 % N_2 and 21 % O_2) and SO_2 (2.46×10^{15} molecules cm^{-3} diluted by N_2).

Before each experiment, a ceramic cup holding particles was placed in the reaction chamber. The particles were treated in a stream of dry air (300 mL min^{-1}) for 30 min to minimize the surface water and impurities (T. Wang et al., 2018a, c). After the pretreatment, the sample was exposed to humidified air (RH = 50 %) to reach moisture saturation, followed by the collection of the background spectrum and then the introduction of a reactant gas for 240 min. The SO_2 concentration was 3.69×10^{13} molecules cm^{-3} in a total flow rate of 100 mL min^{-1}.

The simulated solar irradiation with an actinic flux of 6.51×10^{15} photons $cm^{-2}\,s^{-1}$ was provided by a xenon lamp (TCX-250, Ceaulight, China). The reaction temperature (296.8 K) was controlled by a heater attached to a recirculating cooling water system and determined by a calibration curve introduced previously (T. Wang et al., 2018a). The kinetic parameters involved in the gas- and aqueous-phase oxidation pathways (listed by Sect. 2.2) were corrected by the experimental temperature as much as possible. All exposures were performed in triplicate. The experimental set-ups are displayed by Fig. S4, and the recorded spectra are shown in Figs. S5 and S6.

2.5 Heterogeneous oxidation – acidity and kinetics

The recorded spectra were analysed by referring to the previous literature and the references cited therein (Persson and Vgren, 1996; Peak et al., 1999; Goodman et al., 2001; X. Zhang et al., 2006; Wu et al., 2011; C. Liu et al., 2012; Nanayakkara et al., 2012, 2014; Huang et al., 2016; Ma et al., 2017; W. Yang et al., 2017). In total, six sulfur-containing species can be identified: hydrated SO_2 ($SO_2 \cdot H_2O$), bisulfite, sulfite, solvated sulfate, coordinated

sulfate, and bisulfate, and the assignments are summarized by Table S7. The overlapping bands were further analysed by Gaussian/Lorentzian deconvolution to obtain the product distributions (Fig. S7). The consistent deconvolution procedure was performed for the infrared spectra derived from the repeated experiments.

Because some of the measured ions exist in the surface-coordinated forms or crystalline states, the particle acidity (pH) may not be accurately characterized by the typical proxy methods (Hennigan et al., 2015). Herein, the ionization equilibrium of dissolved SO_2 in the water layers of the particle surface is considered to be associated with particle acidity. As reported, the dissolved SO_2 would transform from $SO_2 \cdot H_2O$ to HSO_3^- and then to SO_3^{2-} as the medium evolves from the extremely acidic to the nearly alkaline (Haynes, 2014; R. Zhang et al., 2015). The relative abundance of $SO_2 \cdot H_2O$ and SO_3^{2-}, as assumed to be equivalent to the relative integral area of their characteristic peaks, is utilized to calculate the particle acidity (more details in Text S3–S2 of the Supplement). The relative abundance of HSO_4^- and SO_4^{2-}, which can be used to calculate the acidity (Rindelaub et al., 2016; Ault, 2020), was not considered by the present study because the characteristic signals of bisulfate cannot be observed in some of the recorded spectra. As noted by Keene et al. (2004) and Hennigan et al. (2015), estimating the pH of airborne aerosol by ion balance may be difficult because it is unable to distinguish between free and undissociated H^+ (e.g. protons associated with HSO_4^- and HSO_3^-). Herein, the relative abundance of $S_{(IV)}$ species is derived from the different infrared absorption signals relevant to atomic sulfur. Thus, the current method is recommended for the pH determination of the humidified gas–solid interface.

Heterogeneous kinetics can be assessed by the reactive uptake coefficient (γ) by assuming a first-order loss of SO_2. The γ for dust-driven heterogeneous reactions can be calculated by

$$\gamma = \frac{\mathrm{d}\left[SO_4^{2-}\right]/\mathrm{d}t}{Z}, \quad (1)$$

$$Z = \frac{1}{4} \times A_s \times [SO_2] \times v_{SO_2}, \quad (2)$$

$$v_{SO_2} = \sqrt{\frac{8RT}{\pi M_{SO_2}}}, \quad (3)$$

where $\mathrm{d}\left[SO_4^{2-}\right]/\mathrm{d}t$ is the rate of sulfate production on the dust surface (ion s^{-1}), A_s is the reactive surface area (m^2), $[SO_2]$ is the experimental concentration of SO_2 (molecules m^{-3}), v_{SO_2} is the molecular velocity of SO_2 ($m\,s^{-1}$), R is the gas constant ($J\,mol^{-1}\,K^{-1}$), T is the experimental temperature (K), and M_{SO_2} is the molecular weight of SO_2 ($kg\,mol^{-1}$). Because the infrared intensity is proportional to the amount of surface product, $[SO_4^{2-}]$ can be translated by the integral area of the sulfate characteristic peaks:

$$\left[SO_4^{2-}\right] = f \times (\text{integral area}), \quad (4)$$

where f is the conversion factor and represents the amount of SO_4^{2-} corresponding to the per-unit integral area. The sulfate production rate of the dust surface can be translated by the calibration curves by mixing weighed Na_2SO_4 with the target particle sample to a set of concentrations (Martin et al., 1987; L. Li et al., 2006; Wu et al., 2011; T. Wang et al., 2020a). The conversion factors are calculated as 1.32×10^{18}, 4.62×10^{17}, 6.97×10^{17}, 8.20×10^{17}, 9.44×10^{17}, and 9.25×10^{17} for NAu, CCa, SWy, KGa, IMt, and natural dust, respectively. Because Na_2SO_4 was thoroughly mixed with the particles, S_{BET} was used to calculate γ.

All samples except SWy presented steady sulfate production potentials over the entire experiment, while the products in SWy increased by reaction time in the beginning and then gradually remained unchanged (Fig. S8). Accordingly, the process in SWy was assessed by the experimental data of the first 30 min of the reaction, and the kinetics of other samples were calculated by the spectra recorded throughout the experiment.

Besides the dust surface drivers, the heterogeneous conversion of SO_2 can be additionally initiated by the gaseous oxidants (O_3, H_2O_2, NO_2, HOCl, HOBr, CH_3OOH, CH_3COOOH, HONO) co-adsorbed with SO_2. Considering that the adsorption of the oxidant onto dust surfaces would produce gas- and particle-phase species (Usher et al., 2003; Tang et al., 2017), the dust-mediated heterogeneous oxidation can be assumed to primarily proceed in the surface water layers. Such an assumption can be experimentally proven as the acceleration of SO_2 oxidation induced by the co-oxidant (e.g. H_2O_2, NO_2, O_3) becomes more significant under higher humidity (Huang et al., 2015; Park et al., 2017; Y. Zhang et al., 2018). Based on the literature (Hanson et al., 1994; Jacob, 2000; Seinfeld and Pandis, 2016; Shao et al., 2019), the γ for dust-mediated heterogeneous reaction can be calculated by

$$\gamma = \left[\frac{1}{\alpha} + \frac{v}{4H^*RT\sqrt{D_a k_{chem}}} \times \frac{1}{f_r}\right]^{-1}, \quad (5)$$

$$k_{chem} = \frac{R_a}{\sum S_{(IV)}}, \quad (6)$$

$$f_r = \coth\frac{r_p}{l} - \frac{l}{r_p}, \quad (7)$$

$$l = \sqrt{\frac{D_a}{k_{chem}}}, \quad (8)$$

where k_{chem} is the pseudo first-order reaction rate constant of the studied $S_{(IV)}$ species (s^{-1}) that is produced at a rate of R_a ($M\,s^{-1}$), f_r is the diffusive correction term comparing the radius of natural dust r_p (m) with the diffuse-reactive length l (m), α is the mass accommodation coefficient of SO_2 (dimensionless), D_a is the aqueous-phase diffusion coefficient

of SO_2 (1.78×10^{-5} m^2 s^{-1} at 296.8 K) (Himmelblau, 1964; Haynes, 2014), H^* is the effective Henry's law constant for the studied $S_{(IV)}$ species (M atm^{-1}) and is jointly determined by the gas–liquid equilibrium of SO_2 and the ionization equilibria of dissolved sulfur species, and R is the gas constant (L atm mol^{-1} K^{-1}). The terms on the right-hand side (RHS) of Eq. (5) show the two contributions to the overall resistance to dust-mediated heterogeneous uptake: mass accommodation at the surface, diffusion, and reaction in surface liquid water layers. The $S_{(IV)}$ species include $SO_2 \cdot H_2O$, HSO_3^-, and SO_3^{2-}.

The sulfate formation rate in the atmosphere can be calculated by the following equations (Jacob, 2000; J. Li et al., 2020).

$$\frac{d\left[SO_4^{2-}\right]}{dt} = \left(\frac{r_p}{D_g} + \frac{4}{v\gamma}\right)^{-1} S_p [SO_2], \quad (9)$$

$$S_p = C \times F \times S_{BET}, \quad (10)$$

where $d\left[SO_4^{2-}\right]/dt$ is the atmospheric sulfate formation rate (μg m^{-3} h^{-1}), r_p is the particle radius (m), D_g is the gas-phase diffusion coefficient of SO_2 (m^2 h^{-1}), v is the molecular velocity of SO_2 (m s^{-1}), γ is the reactive uptake coefficient (dimensionless), S_p is the particle surface area density (m^2 m^{-3}), $[SO_2]$ is the atmospheric SO_2 concentration (μg m^{-3}), C is the dust concentration of 55 μg m^{-3} representative of the common atmospheric condition of China (X. Y. Zhang et al., 2012), F is the mass fraction of clay minerals in the natural dust community (%), and S_{BET} is the BET-specific surface area (m^2 g^{-1}).

2.6 Atmospheric lifetime of SO_2

For the gas- and aqueous-phase pathways, the lifetime of SO_2 (τ) can be calculated by Eq. (11) (Jacob, 2000).

$$\tau = \frac{1}{k_{chem}}, \quad (11)$$

where k_{chem} is the assumed first-order reaction rate constant of the studied $S_{(IV)}$ species (s^{-1}).

For the heterogeneous pathways, the τ can be calculated by Eq. (12) (Clegg and Abbatt, 2001b).

$$\tau = \frac{4}{\gamma v S_p}, \quad (12)$$

where γ is the reactive uptake coefficient (dimensionless), v is the molecular velocity of SO_2 (m s^{-1}), and S_p is the particle surface area density (m^2 m^{-3}), as described by Eq. (10).

The atmospheric lifetime caused by the multiple pathways (τ_{total}) can be estimated by Eq. (13) (Seinfeld and Pandis, 2016).

$$\tau_{total} = \left(\sum \frac{1}{\tau}\right)^{-1} \quad (13)$$

3 Results and discussion

3.1 Driving factors of the dust surface

Correlation analysis is performed to identify the dust surface drivers (Fig. 1), based on which the reaction mechanism of a dust heterogeneous pathway can be better understood (Fig. 2).

The mineral drivers are investigated first (Fig. 1a). Under dark conditions, the sulfate production rate correlates positively with Fe but presents negative dependence against Al. As documented, airborne sulfate was highly associated with Fe-rich dusts, and the heterogeneous reaction of SO_2 can be regarded as a possible explanation (Sullivan et al., 2007). Typical Fe-bearing minerals accelerate the oxidation of $S_{(IV)}$ species by either the surface-active oxygen (O^-) derived from the adsorbed O_2 in an oxygen vacancy or the iron redox cycling initiated by Fe^{3+} from surface acidic media or both (Baltrusaitis et al., 2007; Fu et al., 2007; W. Yang et al., 2016). Conversely, Al_2O_3 presents weaker heterogeneous reactivity than Fe_2O_3 (X. Zhang et al., 2006; W. Yang et al., 2018b; Xu et al., 2021) and may hinder heterogeneous reaction by blocking the active sites of other mineral constituents (T. Wang et al., 2018b). Generally, an Fe-bearing component plays a crucial role in the heterogeneous reaction of SO_2, while the presence of an Al-bearing component directly weakens the dust's reactivity or indirectly decreases the proportion of other active mineral constituents.

The sulfate yield enhanced by solar irradiation associates positively with the abundance of Ti or Al. Transition metal oxides in dust act as a photocatalyst that yields electron–hole pairs, followed by the formation of reactive oxygen species (ROS) such as hydroxyl radicals ($^{\bullet}OH$), superoxides ($O_2^{\bullet-}$), hydroperoxyl radicals ($HO_2^{\bullet}$), and dissociated active oxygen species (O^*) (Chen et al., 2012; Abou-Ghanem et al., 2020; T. Wang et al., 2020b; Sakata et al., 2021). Apart from the site-blocking effect under dark conditions, irradiated Al-bearing constituents additionally facilitate the sulfate formation. Physically, Al-bearing components disperse other efficient mineralogical constituents in the case of agglomeration (Darif et al., 2016). Chemically, sunlight may alter the electronic configuration of α-Al_2O_3, which presented photoactivity in the reported heterogeneous process (Guan et al., 2014). Generally, the kinetic discrepancy between dark reactions and photo-reactions relates primarily to the existence of Ti- and Al-bearing minerals.

No correlation can be observed between the abundance of elements and the sulfate production rate of photo-reaction. The dust with a higher proportion of elemental Ti was reported to exhibit greater reactivity toward SO_2 (Park et al., 2017), NO_2 (Ndour et al., 2009), or O_3 (Abou-Ghanem et al., 2020) in the photochemical processes. However, these results were derived from qualitative comparisons rather than the quantitative analysis performed herein. Analogous to the Al_2O_3 discussed above, semi-conductive metal exhibits dual

behaviours in dark and light reactions. For instance, the iron oxide in dark reactions has great reactivity toward SO_2, whereas that under solar irradiation may present impaired heterogeneous kinetics due to dissolution (Fu et al., 2009). In addition, the heterogeneous reaction on the surface of TiO_2- or Ti-bearing mineral is thermodynamically favoured under dark conditions but depends largely on photocatalysis under solar irradiation (Chen et al., 2012). Due to the complexity of photo-reaction that involves both dark and light reaction mechanisms, the sulfate formation rate of photo-reaction may not be directly linked to particle chemical compositions.

The driving effects of water-soluble ions are further studied (Fig. 1b). Herein, Na^+ and Cl^- are observed to present positive impacts on the sulfate formation under dark conditions. The presence of halite (NaCl) has positive implications for the dust's hydroscopic growth (Y. Wang et al., 2014; Tang et al., 2019), and the moderate surface water provides an efficient medium for the adsorption of gas-phase SO_2 and the ionization of dissolved sulfur species (Rubasinghege and Grassian, 2013). Moreover, there are negative associations between the photo-induced sulfate enhancement and the abundances of Na^+, K^+, and Ca^{2+}. These cations can be hydrolysed by adsorbed water to produce H^+, thereby elevating the particle acidity. In the surface aqueous medium, increased acidity retards the hydrolysis and dissociation of SO_2 (Park et al., 2008; Huang et al., 2015) and inhibits the production of OH by the irradiated dust surface (Zheng et al., 1997; L. Yang et al., 2008; X. Liu et al., 2017). Urupina et al. (2022) reported the positive correlations between secondary dust sulfate and the amount of elemental Na. The results here provide additional insights into the heterogeneous effects of the water-soluble constituents on the dust surface.

Apart from the dust surface drivers and inhibitors, the sulfate radical ($SO_4^{\bullet-}$) may also participate in the heterogeneous event. In the absence of solar irradiation, laboratory studies discovered the non-catalysed SO_2 autoxidation by $SO_4^{\bullet-}$ at the acidic droplet interface (Hung and Hoffmann, 2015; Hung et al., 2018; Chen et al., 2022). With an appropriate humidity and sufficient saline component, there could be an air–liquid interface occurring over the solid dust surface via water uptake (Gaston et al., 2017; Tang et al., 2019; Wu et al., 2020), producing $SO_4^{\bullet-}$. Moreover, on the surface of iron oxide, the $^{\bullet}OH$ derived from a Fenton reaction reacts with SO_4^{2-} to form $SO_4^{\bullet-}$ (Kim et al., 2019; T. Li et al., 2020). The presence of solar irradiation would accelerate the formation of $SO_4^{\bullet-}$ due to the abundant $^{\bullet}OH$ produced via photocatalysis (Antoniou et al., 2018). Generally, the dust surface with a higher proportion of saline components and transition metals may cause the more significant oxidation by $SO_4^{\bullet-}$, especially under solar irradiation with higher ambient humidity and particle acidity.

Based on the correlation analysis, regression analysis can be further performed to predict the surface kinetics by the chemical compositions of dust. Referring to the publication of F. Zhang et al. (2020), we derived an exponential parameterization for the production rate of particle-phase sulfate:

$$\mathrm{SF_{dark}} = M[A]^a[B]^b[C]^c[D]^d[E]^e[F]^f + N, \quad (14)$$

where $\mathrm{SF_{dark}}$ is the yield of SO_4^{2-} on the particle sample of per-unit mass within per-unit time (ions g^{-1} s^{-1}). $[A]$, $[B]$, $[C]$, $[D]$, $[E]$, and $[F]$ are the mass fractions of the element and ions (%). M and N are the constant parameters (dimensionless).

After the statistical procedures by SPSS (version 22.0), we obtained the regression equation for the dark reaction:

$$\mathrm{SF_{dark}}\left(\times 10^{15}\right) = 22.858\,[\mathrm{AI}]^{-0.001}[\mathrm{Fe}]^{0.111} \left[\mathrm{Cl}^-\right]^{0.001}\left[\mathrm{Na}^+\right]^{0.001} - 13.404. \quad (15)$$

Analogously, the discrepancy between the sulfate production rates under dark and illuminated conditions, denoted as $R_{\mathrm{light/dark}}$, can be described by

$$R_{\mathrm{light}} = \mathrm{SF_{light}}/\mathrm{SF_{dark}} = 14.539\,[\mathrm{AI}]^{0.073}[\mathrm{Ti}]^{0.167} \left[\mathrm{Cl}^-\right]^{-0.001}\left[\mathrm{Na}^+\right]^{-0.001}\left[\mathrm{K}^+\right]^{-0.001} \left[\mathrm{Mg}^{2+}\right]^{-0.001} - 3.186. \quad (16)$$

Then,

$$\mathrm{SF_{light}} = \mathrm{SF_{dark}} \times R_{\mathrm{light/dark}}. \quad (17)$$

Because the abundance variation of a water-soluble ion presents significantly less influence on the prediction result relative to the elemental transition metal, the complete regression models can be simplified by merely considering the mineral element abundances:

$$\mathrm{SF_{dark}}\left(\times 10^{15}\right) = 30.880\,[\mathrm{Fe}]^{0.077} - 21.679, \quad (18)$$

$$R_{\mathrm{light/dark}} = 15.581[\mathrm{AI}]^{0.062}[\mathrm{Ti}]^{0.141} - 4.277, \quad (19)$$

$$\mathrm{SF_{light}} = \mathrm{SF_{dark}} \times R_{\mathrm{light/dark}}. \quad (20)$$

The complete and simplified regression models both accurately simulate the experimental data, with all linear slopes approaching 1.0 and all R^2 values larger than 0.995 (Fig. 3). The simplified regression model can be considered the preferred recommendation due to the fewer parameters needed and its greater performance in the photo-reaction prediction. Shang et al. (2010) found that the heterogeneous sulfate production on pristine TiO_2 (Degussa P25) can be accelerated by 8.4 times by the presence of ultraviolet light (365 nm, 350 µW cm^{-2}). Such photo-induced enhancement is comparable with the prediction result (10.2 times) derived from the simplified regression model developed by this study. Additionally, because the chemical composition of a bulk sample may not fully explain the sulfate formation over the dust surface, further study to discuss the model uncertainty is warranted.

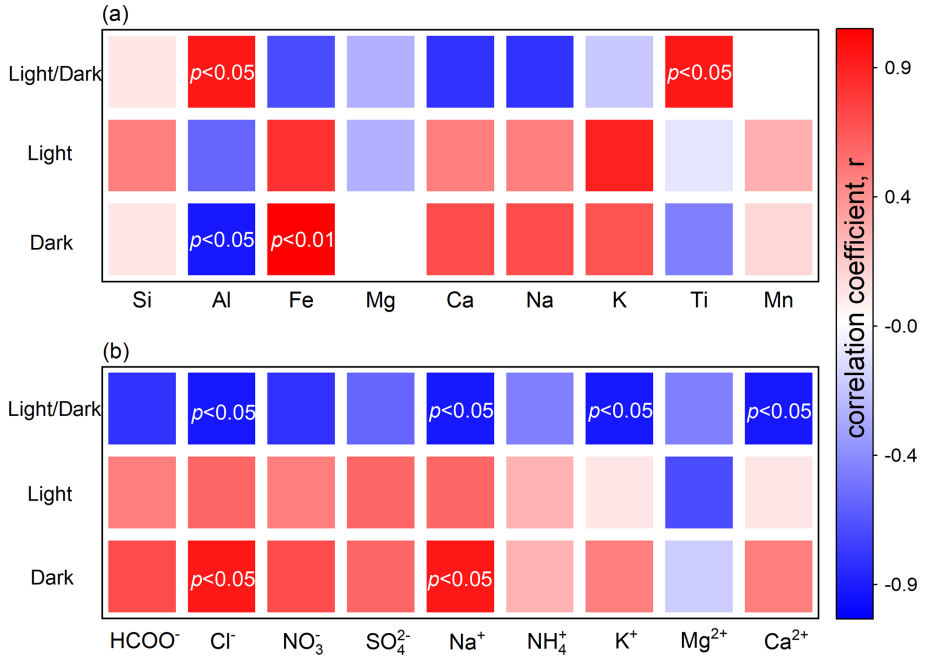

Figure 1. Correlation analysis of the sulfate production rate of the dust surface. Spearman correlation coefficient for the relationship between the rate of sulfate production and the abundance of **(a)** mineral elements or **(b)** water-soluble ions. The significant correlations with p values lower than 0.05 or 0.01 are highlighted by the labels in white.

3.2 Driving force of the dust surface

The driving force of the dust surface can be characterized by a reactive uptake coefficient and particle acidity (Fig. 4, Table S8). Under dark conditions, the γ values are highest for SWy and NAu, followed by IMt and CCa, with that of KGa being lowest. The presence of simulated solar irradiation causes a different rank: IMt > SWy > CCa > NAu > KGa. The γ values of CCa, SWy, KGa, and IMt under dark conditions are, respectively, 1.52, 1.01, 2.94, and 2.30 times greater than those for photo-reactions, reflecting the distinct photocatalytic performances of the clay minerals. Conversely, NAu presents the decreased heterogeneous uptake capacity when exposed to solar irradiation due to its rich abundance of Fe, whose oxides may occur in photo-reductive dissolution in acidic media (Fu et al., 2010; Shi et al., 2012). Comparing the studies performed by the same experimental approach and assessment procedures, these clay minerals are more efficient than the previously concerned mineral dust proxies, including $CaCO_3$ (L. Li et al., 2006; Wu et al., 2011; Y. Zhang et al., 2018), Al_2O_3 (W. Liu et al., 2017), TiO_2 (He and Zhang, 2019), and manganese oxides (T. Wang et al., 2020a) in the heterogeneous production of sulfate under the parallel conditions.

The γ values for the natural dust-driven heterogeneous reactions are calculated as 6.08×10^{-6} under dark conditions and 1.14×10^{-5} under illuminated conditions (Fig. 4a). Within the dataset of authentic dust, the γ for dark reactions is lower than the reported uptake coefficients of Chinese loess (3.0×10^{-5}), Inner Mongolian desert dust (2.41×10^{-5}), Xinjiang sierozem (8.34×10^{-5}), Saharan dust (6.6×10^{-5}), Asian mineral dust (2.54×10^{-5}), Tenger desert dust (4.48×10^{-5}), and Arizona test dust (ATD) (1.92×10^{-5}) under the similar experimental conditions (Usher et al., 2002; Adams et al., 2005; Zhou et al., 2014; Huang et al., 2015). It should be noted that the previous studies measured the net uptake coefficient that quantifies all the heterogeneously adsorbed SO_2, and some of them assessed the oxidations accelerated by surface-adsorbed oxidants (e.g. NO_2, O_3, or H_2O_2). In order to quantify the driving force of the dust surface in the contribution of particle-phase sulfate, $S_{(IV)}$ species were not involved in the current kinetics calculation. Quantitatively, the dust surface drivers are responsible for the atmospheric sulfate formation rates of 0.195 and 0.365 $\mu g\, m^{-3}\, h^{-1}$ during nighttime and daytime, respectively.

Particle acidity is further calculated to discuss the driving force of the dust surface for sulfate formation. After the SO_2 exposure, CCa is the most acidic one, followed by IMt, KGa, and NAu, leaving SWy more neutral. Because no significant correlation can be found between the γ for dust-driven sulfate formation and the pH of reacted clay mineral, the absolute acidity level depends largely on the basic nature of dust. The lowest pH assigned to CCa can be explained by its highest content of elemental Mg relative to the other clays (see Table S6). The Mg-bearing constituents dissolve to Mg^{2+}, which can be further hydrolysed by water to produce H^+, thus accelerating the acidification of particles (Park et al.,

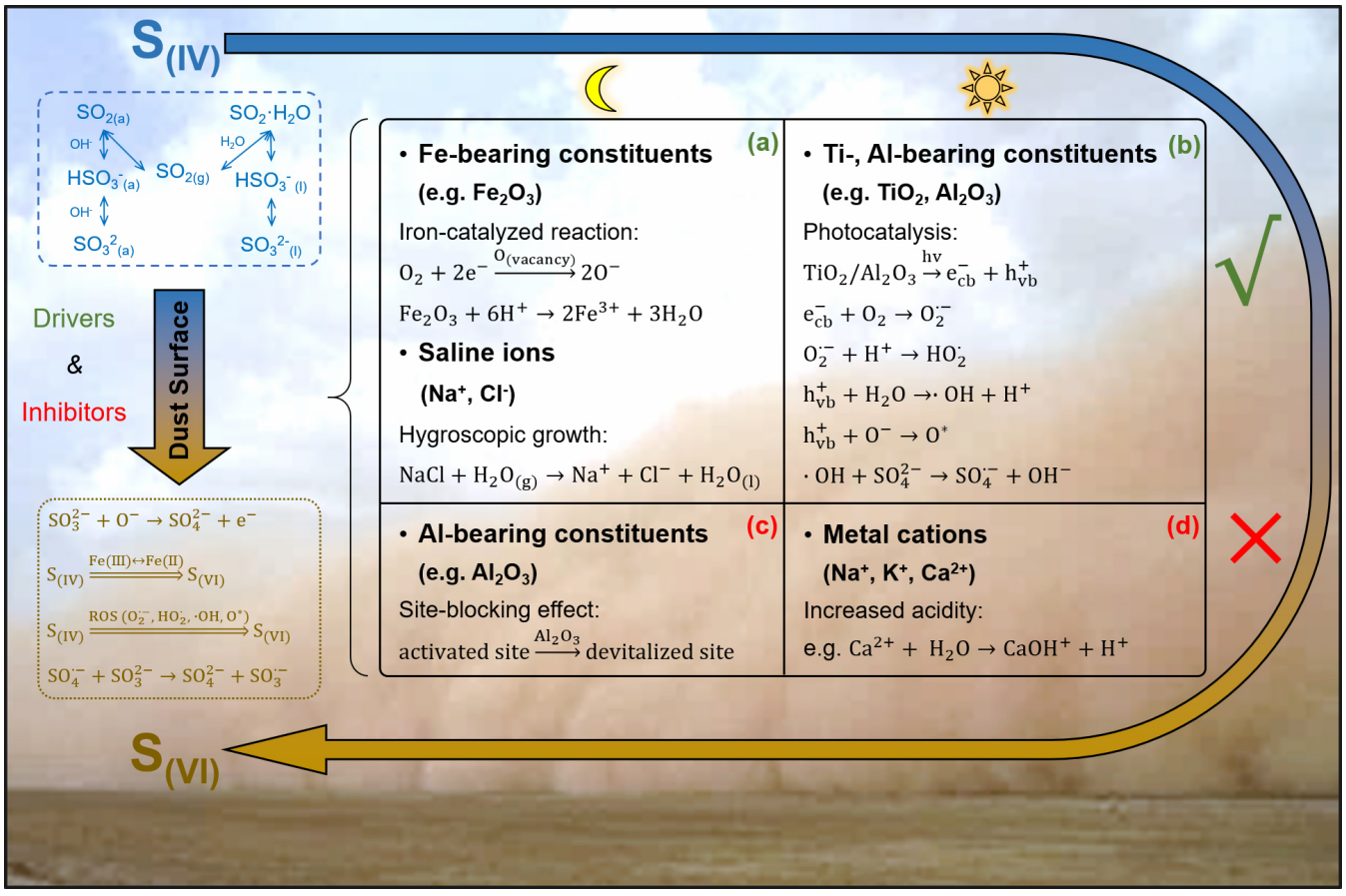

Figure 2. Mechanism illustration of the dust-driven heterogeneous conversion of SO_2. The heterogeneous reaction of airborne SO_2 on a natural dust surface includes the initial adsorption of gas-phase SO_2 and the later conversion of $S_{(IV)}$ species to $S_{(VI)}$ products. The formed $S_{(IV)}$ species include both adsorbed and dissolved SO_2, bisulfite, and sulfite (dashed box in blue). The generation of $S_{(VI)}$ products can be attributed to the surface active oxygen (O^-), Fe(III)–Fe(II) redox cycling, reactive oxygen species (ROS), and sulfate radical ($SO_4^{\bullet-}$) (dotted box in deep yellow). Heterogeneous oxidation is largely influenced by the dust surface drivers and inhibitors, which promote and hinder the heterogeneous procedures, respectively (solid box in black). Dust surface drivers are determined as **(a)** the Fe-bearing constituents and saline ions (Na^+, Cl^-) under dark conditions and **(b)** the Ti- and Al-bearing constituents under solar irradiation. Dust surface inhibitors are identified as **(c)** the Al-bearing constituents under dark conditions and **(d)** the metal cations (Na^+, K^+, Ca^{2+}) under solar irradiation.

2008; Huang et al., 2015). For one clay mineral, its different acidities after dark and light reactions reflect the distinct heterogeneous kinetics. All the studied clays, with the exception of NAu, become more acidic after the photo-reaction than the dark reaction, which can be explained by the photo-induced SO_2 adsorption and sulfate production on these samples. The opposite situation of NAu coincides with the decreased heterogeneous kinetics over its surface by the presence of solar irradiation. Generally, the natural dust presents a particle acidity (pH) of 4.18 after dark reactions and 4.41 after photo-reactions (Fig. 4b). Such results are located within the acidity ranges of dust seeds (3.0–7.0) (Ault, 2020; Pye et al., 2020) and haze aerosols (3.5–4.8) (Ding et al., 2019; Song et al., 2019), suggesting that the dust-driven heterogeneous pathway could affect aerosol acidity to a certain extent.

Figure 5 presents the pH-dependent γ for the natural dust-mediated heterogeneous pathway along with the experimental data of the natural dust-driven heterogeneous pathway. The dust-mediated γ is orders of magnitude lower than the α of SO_2 (~ 0.14 under the experimental temperature of 296.8 K). By definition, α is the probability that a SO_2 molecule striking a liquid surface will finally enter the liquid phase, whereas γ is the sulfate formation rate normalized by the total surface collision rate of SO_2 (Jacob, 2000; Davidovits et al., 2006). That is, γ involves all the uptake processes, including the mass accommodation at the surface (Seinfeld and Pandis, 2016). Moreover, unlike the pH-independent α, γ varies with pH, somewhat coinciding with the evolution of dissolved sulfur species that can be quantitatively described by the H^* of SO_2. The γ values of H_2O_2, CH_3OOH, and CH_3COOOH are pH-independent under spe-

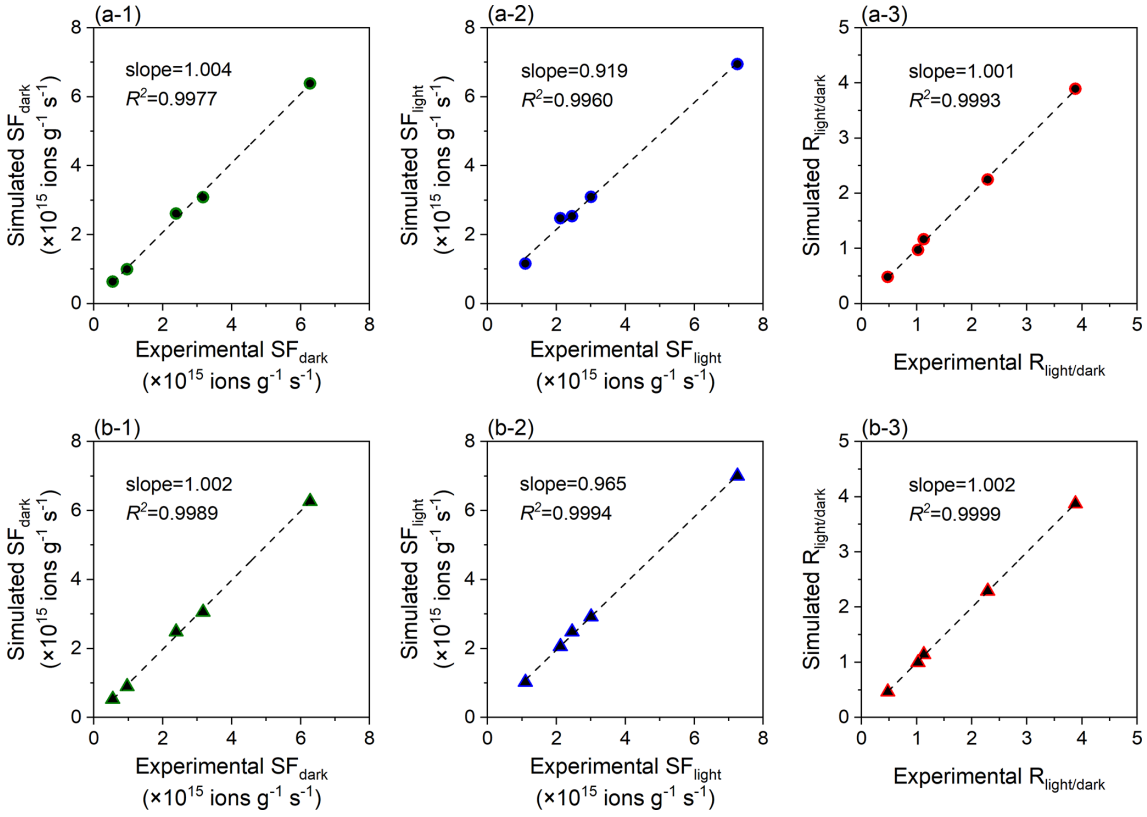

Figure 3. Regression analysis of the sulfate production rate of the dust surface. Linear relationships between the experimental SF_{dark}, SF_{light}, and $R_{light/dark}$ and those simulated by the **(a)** complete and **(b)** simplified regression models. The unit of SF (ions g^{-1} s^{-1}) indicates the amount of SO_4^{2-} formed on the particle sample of per-unit mass per unit time, and $R_{light/dark}$ indicates the ratio of SF values in the presence and absence of simulated solar irradiation.

cific conditions in relation to the acid-catalysed rate-limiting steps relevant to these peroxides (Lind et al., 1987; T. Liu et al., 2021). Generally, the dust-mediated heterogeneous γ is largely determined by the diffusion and reaction processes in the water layers of the dust surface, as characterized by the second item on the RHS of Eq. (5).

The dust-mediated heterogeneous sulfate formation is primarily contributed by the surface-adsorbed H_2O_2 below the nocturnal pH of 5.50 or the diurnal pH of 5.27. When the acidity exceeds the thresholds, the dust-mediated pathway would be kinetically dominated by NO_2 and O_3 during nighttime or HOBr and HOCl during daytime. Comparing the γ values with the same acidity, the dust-driven pathway appears to be more efficient than the dust-mediated one, thus having the possibility of accounting for more secondary sulfate aerosols. In the following sections, the oxidation of SO_2 mediated or driven by the natural dust would be set as the typical dust-mediated and dust-driven heterogeneous reactions to compare them with the widely documented gas- and aqueous-phase pathways.

3.3 Comparison of atmospheric oxidation pathways

Figure 6 compares the sulfate formation rates of diverse atmospheric oxidation pathways with a newly developed comparison model. Based on the parameterization scheme in the model and the experimental results discussed above, the total sulfate formation rates are summed to 0.795 μg m^{-3} h^{-1} during nighttime and 5.179 μg m^{-3} h^{-1} during daytime under the acidity of natural dust (Fig. 6a and e). The higher sulfate flux during daytime can be explained by the photo-increased oxidation channels, oxidant concentrations, heterogeneous reactivity, and the elevated particle acidity that facilitates the TMI catalysis. It is worthwhile mentioning that the nocturnal sulfate concentration was reported to approach or exceed the subsequent diurnal level, as explained by the higher nocturnal humidity facilitating the liquid oxidations or the lower boundary layer at night causing the adverse diffusion conditions (J. Liu et al., 2017; Tutsak and Koçak, 2019; S. Li et al., 2020). Meteorological factors like humidity are not considered by the current model, which emphasizes the comparison of diverse pathways through the kinetic regime. The estimated sulfate fluxes are generally lower than some published data derived from the same concentration of SO_2 (40 ppb)

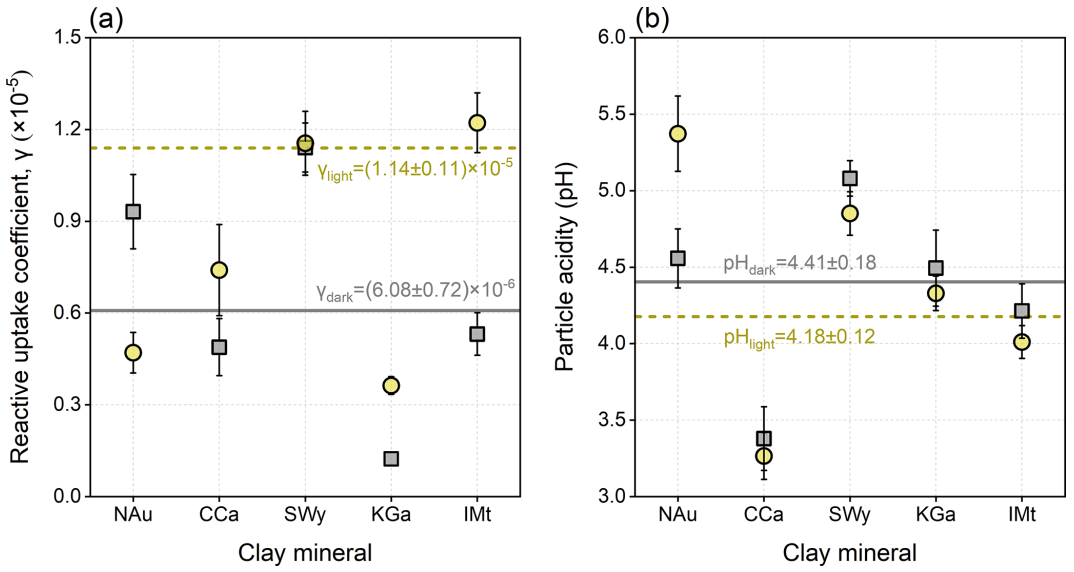

Figure 4. Analysis results of the in situ infrared spectra recorded for the heterogeneous reaction of SO_2 on clay minerals and natural dust. **(a)** Reactive uptake coefficients (γ) for the heterogeneous formation of sulfate. **(b)** Particle acidity (pH) of the reacted particle samples. The dark (grey square) and light (yellow circle) conditions were both considered. Dots represent the results of clay minerals, and those of natural dust are showed by the lines. All error bars represent 1 SD.

because the gas- and aqueous-phase parameters here are corrected by the experimental temperature (296.8 K) rather than the much lower level (271 K) used previously (Cheng et al., 2016; Gen et al., 2019; T. Liu et al., 2020; Su et al., 2020; X. Wang et al., 2020; T. Liu et al., 2021). Considering that some kinetic parameters were experimentally determined under room temperature with the lack of temperature dependence, uncertainties may exist in the discussion on cold environments. The current sulfate formation is assessed near room temperature, which is pertinent to the nature of sandstorms occurring during late spring and early summer in East Asia (Wu et al., 2020; Ren et al., 2021).

During nighttime, the gas-phase, aqueous-phase, and heterogeneous pathways explain 31.6 %, 39.8 %, and 28.6 % of secondary sulfate, respectively (Fig. 6b). The diurnal contribution proportions of gas-phase (45.5 %) and aqueous-phase pathways (41.4 %) exceed their nocturnal levels, thus lowering the heterogeneous proportion to 13.1 % during daytime (Fig. 6f). Although the heterogeneous sulfate yield during nighttime is lower than that during daytime (see Sect. 3.2), the nocturnal heterogeneous process accounts for the higher proportion of secondary sulfate. The diurnal sulfate formation rates of gas-phase, aqueous-phase, and heterogeneous pathways are, respectively, 9.4, 6.8, and 3.0 times greater than the nocturnal levels, indicating that the oxidations in gaseous and liquid media could be more kinetically susceptible to the occurrence of sunlight than those relevant to the humidified gas–solid interface. In gas-phase oxidation, OH is the predominant oxidant, followed by CIs, while NO_3 contributes little. In aqueous-phase oxidation, TMI-O_2 and H_2O_2 play crucial roles in the conversion of SO_2, coinciding with the reported results (Fan et al., 2020; Song et al., 2021). In addition, there are lower contributions from the NO_2 during nighttime and the HOBr, T^*, and $P_{NO_3^-}$ during daytime. The heterogeneously formed sulfate is mostly ascribed to the dust-driven pathway rather than the dust-mediated one. In comparison, the sulfate contribution proportions of the studied dust heterogeneous oxidation are comparable with those obtained by the OBM model (30.6 % for nighttime and 19.4 % for daytime) (Xue et al., 2016), the revised GEOS-Chem model (20 %–30 %) (Tian et al., 2021), and the WRF-CMAQ model (up to 12 %) (K. Wang et al., 2012). While the uptake coefficients used in the previous studies are generally greater than the present experimental results, more pathways are implemented in the current comparison model, thereby causing the parallel comparison results. By contrast, the AMAR model highlighted the dust's photocatalytic surface that contributes remarkable secondary sulfate (> 50 %) under the constraint of simulation conditions (Yu et al., 2017).

In dust-mediated heterogeneous oxidation, H_2O_2 is the most efficient oxidant, followed by the nocturnal NO_2 and diurnal hypohalous acids (HOBr, HOCl) responsible for less secondary sulfate (Fig. 6c, g). The dust-driven heterogeneous sulfate formation is mainly attributed to IMt, which has the largest proportion in the dust community, followed by NAu and SWy with relatively significant contributions by heterogeneous sulfate formation (Fig. 6d, h). The nocturnal and diurnal sulfate fluxes of the natural dust-driven heterogeneous pathway are, respectively, 5.8 and 1.2 times greater

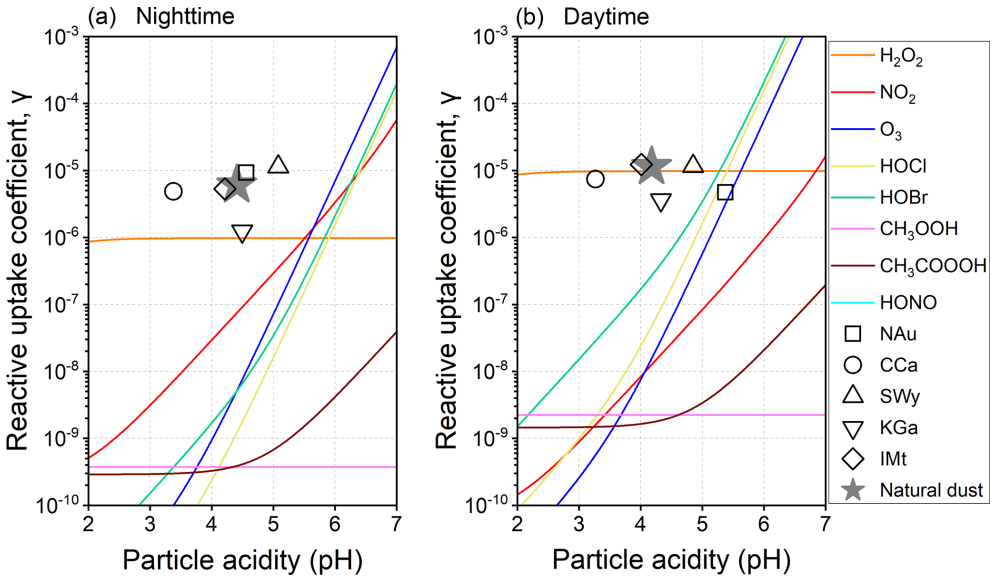

Figure 5. Particle acidity-dependent reactive uptake coefficients (γ) for the dust-mediated and dust-driven heterogeneous pathways. The dust-mediated pathway can be induced by the surface oxidants co-adsorbed with SO_2, including hydrogen peroxide (H_2O_2), nitrogen oxide (NO_2), ozone (O_3), hypochlorous acid (HOCl), hypobromous acid (HOBr), methyl hydroperoxide (CH_3OOH), peroxyacetic acid (CH_3COOOH), and dissolved nitrous acid (HONO). The dust-driven pathway can be induced by the heterogeneous drivers (transition-metal-bearing components and water-soluble ions) on natural dust and clay minerals – NAu, CCa, SWy, KGa, and IMt.

than those of the natural dust-mediated one. Hence, the heterogeneous sulfate formation is primarily ascribed to the dust surface drivers rather than the surface-adsorbed oxidants, as experimentally proven by the laboratory studies concerning the heterogeneous SO_2 oxidation on authentic dusts accelerated by the presence of NO_2 (Park et al., 2017), O_3 (Park et al., 2017), or H_2O_2 (Huang et al., 2015). The kinetic discrepancy between the dust-mediated and dust-driven heterogeneous pathways is more significant during nighttime than daytime. In the estimation, H_2O_2 is the predominant dust-mediated oxidant, and its concentration becomes lower under weaker sunlight. The dust-mediated contribution during nighttime is thus relatively small by the presence of the relatively low H_2O_2 concentration. In general, when investigating the heterogeneous process on dust particles, particle variables could be more important than gas variables in elucidating the reaction characteristics and atmospheric implications.

Figure 7 summarizes the particle acidity-dependent sulfate formation rates of gas-phase, aqueous-phase, and heterogeneous pathways. Relative to the pH-independent gas-phase process, the aqueous-phase oxidation becomes relatively productive under the extremely acidic and near-neutral situations but fails to support the rapid sulfate formation within the pH range of 4–5 (minima at 4.85 for nighttime and 4.55 for daytime), which overlaps with the acidity range of the weak dust-mediated heterogeneous pathway. The significant sulfate formation in the acidic medium is primarily contributed by the TMI-O_2 pathway where the concentrations of TMIs and H^+ keep increasing as the aerosol water becomes more acidic. When pH > 5.0, the sulfate formation rate increases with elevated pH, in step with the evolution of the concentration of dissolved sulfur species. Noticeably, the pH range of 4–5 involves the acidity of the aged natural dust and overlaps with that of the common haze aerosols, implying that the dust surface drivers have profound impacts on the secondary sulfate burst in a highly polluted environment (Ding et al., 2019; Song et al., 2019). The important role of dust in sulfate formation was confirmed by atmospheric observation research. For example, secondary sulfate was observed to accumulate on the dust-dominant super-micron particles collected in the North China Plain, and the mass fraction of coarse-mode sulfate dramatically increased during the evolutionary stages of haze episodes (Xu et al., 2020). Within the entire pH range, the aqueous-phase pathway is more active than the dust-mediated heterogeneous one in contributing to secondary sulfate.

Figure 8 compares the lifetimes of SO_2 influenced by the diverse atmospheric oxidation pathways. Calculations of lifetimes can be useful in estimating how long the SO_2 is likely to remain airborne before it is removed from the atmosphere (Seinfeld and Pandis, 2016). Theoretically, the lifetime of SO_2 determined by heterogeneous reaction is negatively correlated with γ and S_p, and S_p is positively associated with the concentration and S_{BET} of dust as, respectively, described by Eqs. (12) and (10). As a result, the dust with greater heterogeneous reactivity, higher atmospheric loading, or larger S_{BET} is prone to causing the shorter lifetime. During nighttime, IMt causes the shortest SO_2 lifetime (46.90 d) due to its

highest concentration relative to the other clay minerals. The relatively large heterogeneous uptake capacity of NAu and SWy links to the second- and third-shortest SO_2 lifetimes (221.30 and 260.12 d, respectively). On the other hand, the weakest heterogeneous reactivity of KGa leads to the second-longest lifetime (1758.65 d), and the longest result caused by CCa (2256.25 d) can be interpreted by its lowest S_{BET} that causes the lowest S_p. The presence of solar irradiation alters the lifetime ranking, IMt (20.39 d) < SWy (256.96 d) < NAu (437.85 d) < KGa (597.54 d) < CCa (1488.46 d), as influenced by the different photo-activities of the clay minerals. The heterogeneous drivers of the natural dust surface are comparable with TMI-O_2 in the loss of SO_2, and both of them function as the most important lifespan influencers in the absence of sunlight (Fig. S9a). During daytime, the natural dust-driven pathway is only next to the oxidations induced by OH, TMI-O_2, and H_2O_2 (Fig. S9b). The comparison results of the lifetime agree well with those of the sulfate formation rate (Fig. 6), illustrating that the heterogeneous drivers of the dust surface are somewhat responsible for altering the concentrations of gas-phase and particulate sulfur species.

Gas- and aqueous-phase pathways serve as the most significant influencers of the diurnal lifespan of SO_2, followed by the dust-driven heterogeneous pathway, while during nighttime these three present closer impacts (Fig. S10). The atmospheric lifetimes of SO_2 induced by the considered atmospheric oxidation pathways are calculated as 6.17 d during nighttime and 0.99 d during daytime. Neglecting dust heterogeneous pathways may lengthen the SO_2 lifespans to 10.27 and 1.12 d in the absence and presence of solar irradiation, respectively. Analogously, scientists obtained the shorter lifetime of SO_2 from the climate model after considering the heterogeneous reaction occurring on volcanic ash particles (Zhu et al., 2020). Clay minerals are more concentrated in the troposphere than volcanic ash and thus have more significant impacts on the removal of atmospheric SO_2.

3.4 Sensitivity analysis

The aforementioned calculations set the concentration of natural dust to 55 $\mu g\,m^{-3}$. In contrast to the common atmospheric loading, the burst ofvsandstorm was normally accompanied by the quickly elevated dust concentration of up to thousands of micrograms per cubic metre (G. Li et al., 2021; Yin et al., 2021; Filonchyk, 2022). It would be meaningful to estimate the heterogeneous contributions in the dust-rich environments. Theoretically, dust concentrations within the ranges of 72–770 $\mu g\,m^{-3}$ during nighttime and 24–260 $\mu g\,m^{-3}$ during daytime could cause the extra sulfate formation of 0.3–3.0 $\mu g\,m^{-3}\,h^{-1}$ (Fig. 9a), in line with the acknowledged range of the missing sulfate formation rate (Cheng et al., 2016; T. Liu et al., 2020), which was found to be positively correlated with PM concentration as well (Cheng et al., 2016). Therefore, the heterogeneous reaction of SO_2 on the dust surface is a considerable sulfate formation pathway and may evolve into the missing sulfate source in the atmosphere.

The occurrence of sandstorms, particularly during nighttime, aggravates the sulfate pollution in the coarse aerosol mode (Fig. 9b). For instance, the dust concentration of 200 $\mu g\,m^{-3}$, which approaches the PM_{10} level in North China in March 2021 (Yin et al., 2021), could heterogeneously explain 44.9 % of the secondary sulfate during nighttime as well as 29.6 % during daytime. It is worthwhile noting that the heterogeneous contribution proportion is susceptible to the evolution of a relatively low dust concentration, and a further increase in dust loading will not significantly elevate the heterogeneous proportion, resulting in a plateau (nighttime) or decrease (daytime) under severe dust pollution. In fact, the increased dust concentration facilitates the aqueous-phase TMI-O_2 pathway and dust-mediated and dust-driven heterogeneous reactions but presents negative impacts on the others by the removal of gaseous oxidants over the dust surface. The unsusceptible response to dust concentration, as shown by Fig. 9b, is related to the increased sulfate contributions from TMI-O_2. Unlike the TMI-derived oxidation and dust-driven pathway receiving constant positive feedbacks from the increased dust concentration, the dust-mediated pathway is somewhat affected by the decreased oxidants adsorbed on the dust surface. Since the importance of the dust-mediated pathway is more significant during daytime than nighttime, there is a negative correlation between the high dust concentration and heterogeneous contribution proportion in the presence of solar irradiation.

The increased dust concentration, in fact, not only facilitates the heterogeneous process by providing more reactive surfaces, but also affects the gas- and aqueous-phase reactions by altering the atmospheric abundances of reactive species, as explained below. The evolution of dust pollution from slight to heavy conditions would cause the loss of various gaseous oxidants by heterogeneous uptake, and therefore the gas- and aqueous-phase sulfate fluxes, except those induced by TMI-O_2, decrease against dust concentration (Bian and Zender, 2003; Tang et al., 2017). Furthermore, the dissolution of mineral constituents produces TMIs in aerosol liquid media (Alexander et al., 2009; Shao et al., 2019), and the irradiated mineral dust was reported to emit gaseous ROS by surface photocatalysis (Dupart et al., 2012; Chen et al., 2021). Herein, the studied oxidation pathways are distinguished by their contribution proportions (Fig. 9c and d). The contribution proportions of OH and H_2O_2 decrease against dust loading, whereas the importance of TMI-derived oxidation and the dust-driven pathway become more significant as the dust concentrates. The contribution proportion assigned to the dust-mediated process increases with dust concentration at first and then decreases. While the increased dust loading provides more physical space for the dust-mediated reactions, the simultaneously decreased gas-phase oxidants restrain the accumulation of particle-phase oxidants.

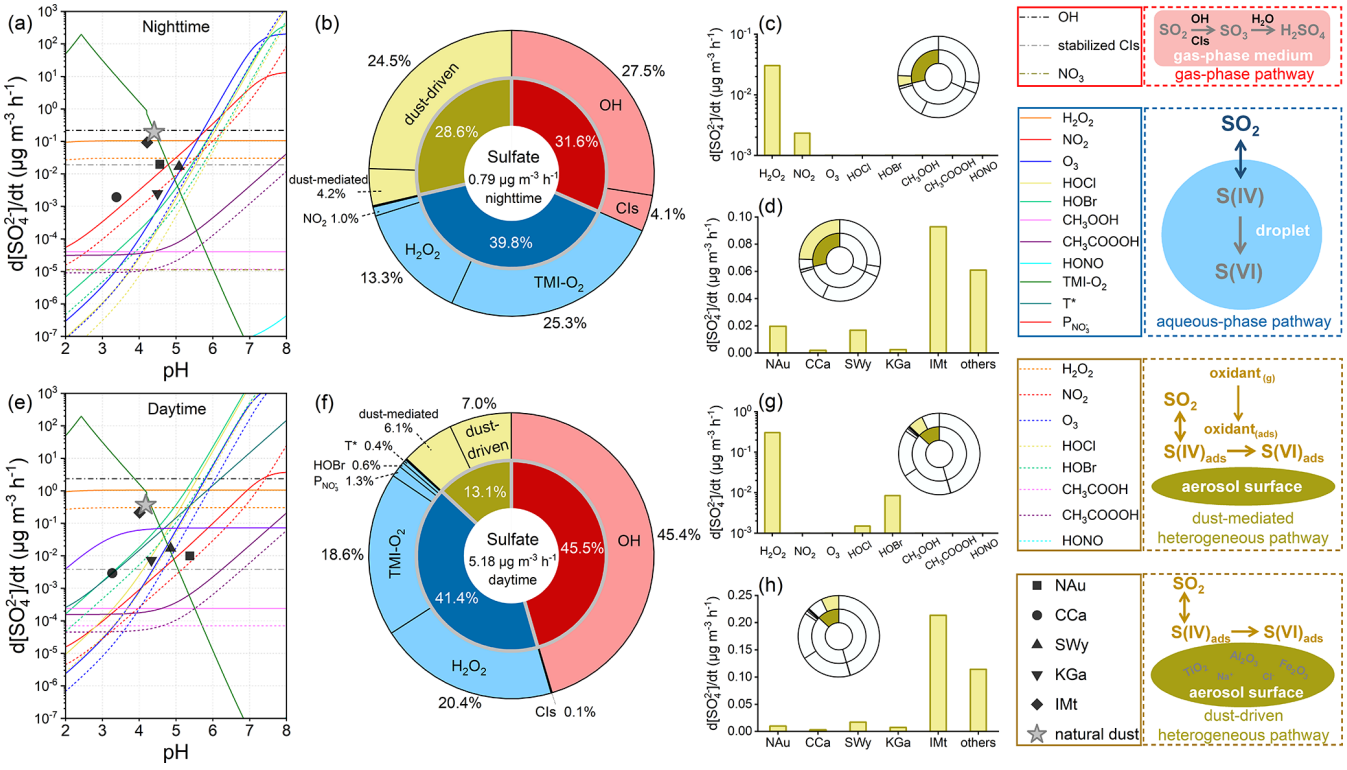

Figure 6. Contributions of diverse atmospheric oxidation pathways to secondary sulfate aerosols. Gas-phase oxidation can be induced by the hydroxyl radical (OH), stabilized Criegee intermediates (CIs), as well as nitrate radical (NO_3) only for nighttime. Aqueous-phase oxidation can be induced by hydrogen peroxide (H_2O_2), NO_2, O_3, HOCl, HOBr, CH_3OOH, CH_3COOOH, HONO, TMI-O_2, and the T^* and $P_{NO_3^-}$ only for daytime. Dust-mediated heterogeneous oxidation can be initiated by the surface oxidants (H_2O_2, NO_2, O_3, HOCl, HOBr, CH_3OOH, CH_3COOOH, HONO) co-adsorbed with SO_2. Dust-driven heterogeneous oxidation can be ascribed to the heterogeneous drivers (transition-metal-bearing components and water-soluble ions) on the surfaces of natural dust and clay minerals – nontronite (NAu), chlorite (CCa), montmorillonite (SWy), kaolin (KGa), and illite (IMt). The **(a–d)** nighttime and **(e–h)** daytime conditions were distinguished by the different parameterizations. **(a, e)** Particle acidity-dependent sulfate formation rates of the diverse atmospheric oxidation pathways. The elements' colours and shapes are characterized by the legends in solid boxes. **(b, f)** Quantified sulfate contribution proportions of the studied gas-phase (red), aqueous-phase (blue), and heterogeneous (yellow) reaction pathways. Sulfate formation rates of the dust-mediated and dust-driven pathways during **(c–d)** nighttime and **(g–h)** daytime. The effects of ionic strength on the aqueous-phase oxidation were not taken into account. The dust concentration was set to 55 $\mu g\,m^{-3}$, representative of the common atmospheric condition of North China (X. Y. Zhang et al., 2012). The panels in dashed boxes right of the legends illustrate the primary physical–chemical processes of atmospheric sulfate formation. More parameterization and methodology details can be found in Texts S2–S4 of the Supplement and Sect. 2.1–2.5 of the main content.

The atmospheric lifetime of SO_2 is also affected by the concentration of dust. As shown by Fig. 10a, the lifespan of airborne SO_2 during nighttime is higher than that during daytime, and both of them decrease against dust concentration. Analogous to the heterogeneous contribution proportion (Fig. 9b), the lifespan of SO_2 is more susceptible to the variation of dust concentration in clean and slightly polluted environments than that under heavily polluted conditions. The mild dust pollution, especially its level variations, should be given more attention. The heterogeneous loss of SO_2 by the dust surface was normally evaluated against the gas-phase loss by OH (Ullerstam et al., 2003; Adams et al., 2005; L. Li et al., 2006; Huang et al., 2015; Ma et al., 2018). Current estimation indicates that the airborne dust with the concentration of 45 $\mu g\,m^{-3}$ during nighttime or 91 $\mu g\,m^{-3}$ during daytime can be regarded as comparable with OH in controlling the removal of SO_2 (Fig. 10b). Such dust concentrations are sometimes common in the troposphere, especially during the dust storm periods (G. Li et al., 2021; Yin et al., 2021; Filonchyk, 2022) or near the dust source regions (Ke et al., 2022). Therefore, the heterogeneous loss of SO_2 by the airborne dust surface may have a similar magnitude to the main gas-phase loss process and can be taken as an important sink for SO_2.

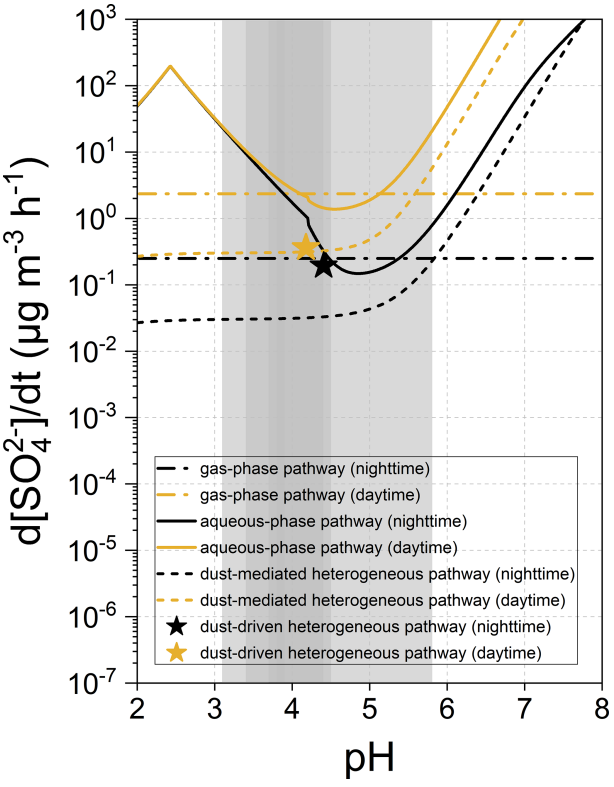

Figure 7. Formation rate of sulfate attributed to the gas-phase, aqueous-phase, and dust heterogeneous pathways as a function of particle acidity (pH). Grey areas indicate the pH ranges of the polluted particulate matters, with darker ones being more common (Ding et al., 2019).

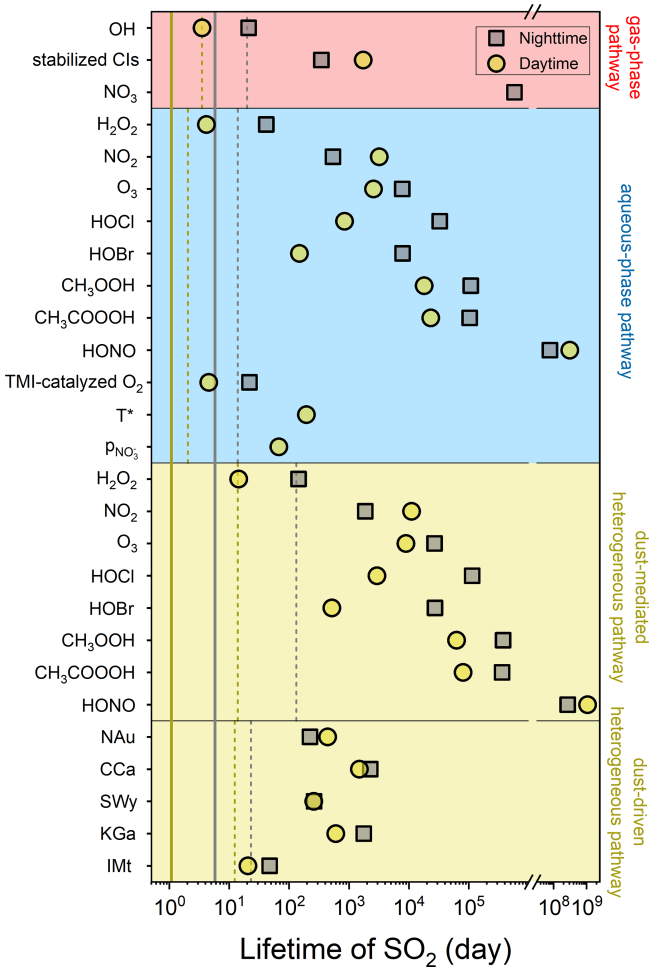

Figure 8. Atmospheric lifetimes of SO_2 induced by the diverse sulfate formation pathways. Both nighttime (grey square) and daytime (yellow circle) conditions were considered. The lifetimes of SO_2 caused by gas-phase, aqueous-phase, and dust heterogeneous pathways are displayed by the dashed lines. The atmospheric lifetimes of SO_2 induced by all the studied oxidation pathways are presented by the solid lines. The effects of ionic strength on the aqueous-phase SO_2 oxidation were not taken into account. The dust concentration was set to 55 $\mu g\,m^{-3}$ to reflect the common atmospheric condition of North China. More methodology details can be found in Sect. 2.6 of the main content.

3.5 Uncertainty analysis

The contribution proportion of dust heterogeneous oxidation could be overestimated or underestimated when considering the uncertainty factors. Herein, the joint impacts of ionic strength (I) and aerosol liquid water content (ALWC) on the aqueous-phase oxidation and the kinetic comparison between microdroplet interfacial oxidation and dust-driven heterogeneous oxidation are discussed to further understand the atmospheric relevance of the heterogeneous drivers for the dust surface under the complex atmospheric conditions.

The aqueous-phase oxidation of SO_2 by H_2O_2, O_3, NO_2, and TMI-O_2 was quantified under different I–ALWC settings. First, the sulfate formation rate was calculated as a function of ionic strength under the studied ALWC of 300 $\mu g\,m^{-3}$ (Fig. S11). TMI-O_2 and H_2O_2 dominate the liquid oxidation, while the impacts of NO_2 and O_3 only slightly peak at $\sim$ 1.0 M during nighttime. Specifically, during nighttime, TMI-O_2 dominates the sulfate formation under the relatively low ionic strength, while the contribution of H_2O_2 exceeds that of TMI-O_2 over the ionic strength of 0.028 M. During daytime, H_2O_2 is the predominant oxidant within the studied ionic strength range. Relative to the ionic strength-free calculations, the aqueous oxidation could be weakened by the ionic strength lower than 17.8 M during nighttime or 14.3 M during daytime. Such values can be taken as criteria to distinguish the overestimation or underestimation of liquid kinetics under the ALWC of 300 $\mu g\,cm^{-3}$, which was widely used to characterize the haze events in North China (Cheng et al., 2016).

The joint influences of I and ALWC were further considered (Fig. 11). At each ionic strength, sulfate formation rate associates positively with ALWC. At each ALWC, the increase in ionic strength hinders the aqueous oxidation at first and then facilitates this process, as a consequence resulting in

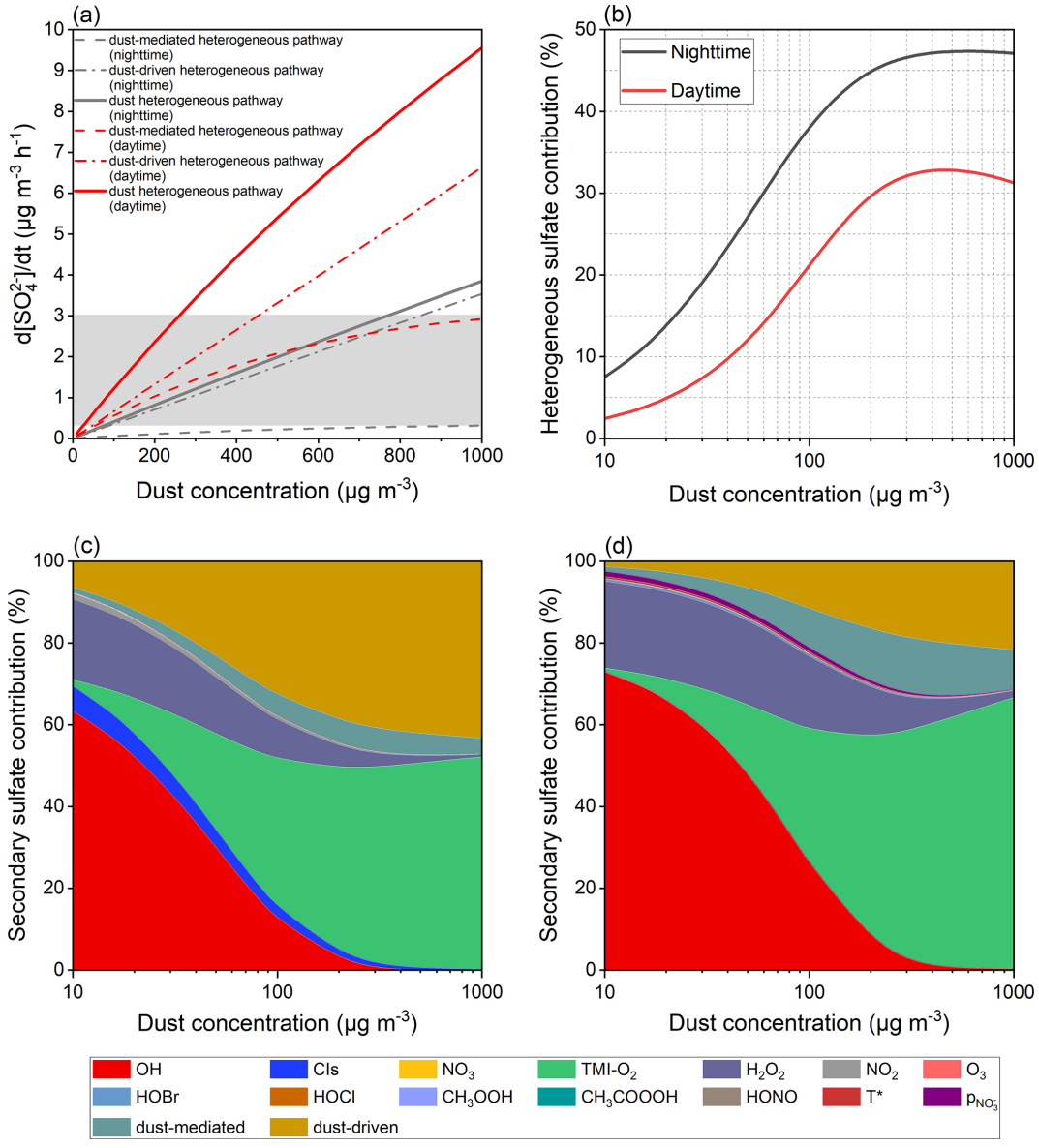

Figure 9. Sensitivity tests of the sulfate formation rate to dust concentration. **(a)** Sulfate formation rate of diverse dust-related heterogeneous pathways as a function of dust concentration. The grey area suggests that the missing sulfate formation rate ranges from 0.3 to 3 $\mu g\,m^{-3}\,h^{-1}$ as a reference (Cheng et al., 2016; T. Liu et al., 2021). **(b)** Heterogeneous sulfate proportion varying with dust concentration. Secondary sulfate contributions attributed to the studied oxidation pathways during **(c)** nighttime and **(d)** daytime.

a threshold line distinguishing the negative or positive effects of ionic strength, as presented by Fig. 11a and b. Furthermore, the I–ALWC relationships of California, USA (Stelson and Seinfeld, 1981), Beijing, China (Song et al., 2021), Mexico City, Mexico (Volkamer et al., 2007; Hennigan et al., 2015), and the nine cities of Germany (Scheinhardt et al., 2013) were found to be located left of the thresholds, indicating the negative effect of ionic strength under the investigated scenarios (Fig. 11c). Calculated by the reported I–ALWC relationships, the dust-mediated pathway contributes 4.3 %–20.1 % of the secondary sulfate during nighttime and 6.8 %–22.0 % during daytime, and the dust-driven pathway accounts for, respectively, 29.1 %–41.6 % and 9.9 %–12.4 % of the sulfate formation in the absence and presence of sunlight (Fig. 11d). Therefore, the heterogeneous contribution proportions in the complex atmospheric environments can be even higher than those estimated by this study.

Besides the humidified gas–solid interface, the gas–liquid interface of microdroplets is another type of medium that supports the heterogeneous formation of sulfate. The oxidation of SO_2 was found to proceed at the interfacial layer of a droplet with higher kinetics than the bulk process (Jayne

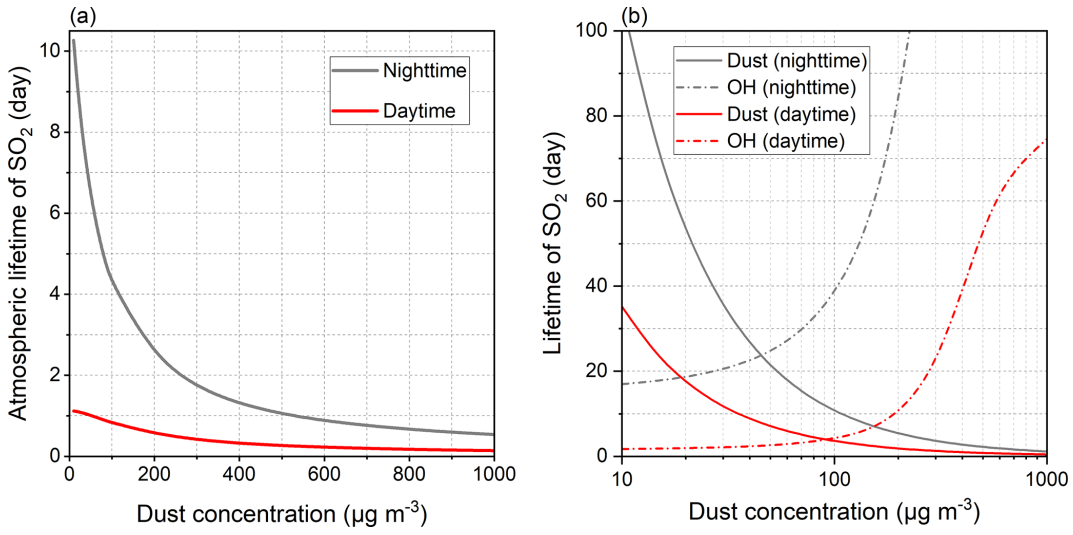

Figure 10. Sensitivity tests of SO_2 lifetime to dust concentration. **(a)** Atmospheric lifetime of SO_2 induced by all the studied pathways varying with dust concentration. **(b)** Comparison between the SO_2 lifetimes ascribed to the dust heterogeneous pathway and OH-initiated gas-phase oxidation.

and Davidovits, 1990). Recently, the interfacial roles of O_2 (Hung and Hoffmann, 2015; Hung et al., 2018; Chen et al., 2022), NO_2 (Liu and Abbatt, 2021; Yu, 2021), and Mn^{2+} (H. Zhang et al., 2021; W. Wang et al., 2021; T. Wang et al., 2022) have been quantitatively described. Figure 12 compares the dust-driven heterogeneous pathway with the documented gas–liquid interfacial oxidations. As reported by Hung et al. (2015, 2018), the acidic droplet interface favours the non-catalysed oxidation by the presence of sufficient $SO_3^{\bullet-}$ and $SO_4^{\bullet-}$ when pH < 4.0, which can be further explained by the structure differences of water at the interface and in the bulk phase. Recently, Chen et al. (2022) reevaluated the sulfate formation by interfacial O_2 within the pH range of 3.5–4.5 and discovered the positive dependence on ionic strength. The oxidation of SO_2 by interfacial NO_2 displays a similar pH dependence to that which occurs in bulk solution. The secondary sulfate contributed by interfacial Mn^{2+} is associated positively with particle acidity. Generally, the O_2 at the acidic interface dominates the oxidation when pH < 4.0, whereas at pH > 4.0, the interfacial oxidation is primarily controlled by Mn^{2+}. Comparing the sulfate formation rates under the same aerosol acidity, the dust surface drivers generally present greater reactivity than the interfacial NO_2 and O_2. Under the ionic strength of 40 M, the reactivity of interfacial O_2 can be regarded as equivalent to that of the dust surface drivers during nighttime. Interfacial Mn^{2+} exceeds the dust surface drivers through the kinetic regime. For instance, the Mn^{2+}-catalysed oxidation characterized by W. Wang et al. (2021) is 6.5 or 1.7 times more efficient than the dust-driven pathway in sulfate formation during nighttime or daytime, respectively.

The dust-driven heterogeneous pathway here was investigated by the infrared technique focusing on the bulk particle sample rather than air-suspended particles. Up to now, the microscale effects of dust particles have not been systematically studied. Suspended ATD was the subject of a smog chamber study, and its heterogeneous reactivity toward SO_2 was characterized by the net uptake coefficient of 1.71×10^{-6} under dark conditions (Park and Jang, 2016). Such a kinetic constant is approximately 1 order of magnitude higher than those obtained from the film-based flow tube tests ($\sim 1.75 \times 10^{-7}$) under the parallel experimental conditions (Y. Zhang et al., 2019). Therefore, in the atmosphere, dust surface drivers may kinetically approach the microdroplet interface in the removal of SO_2 and the formation of sulfate.

4 Conclusions and implications

This study attempted to deeply understand the importance of heterogeneous oxidation, particularly that induced by dust surface drivers, in the loss of airborne SO_2 and formation of sulfate aerosols. Laboratory research was performed first to investigate the heterogeneous driving factors and driving forces. Based on the correlation and regression analysis, transition metal elements, particularly Fe for dark conditions and Al and Ti for photo-reaction, were determined to dominate the heterogeneous oxidation, while water-soluble ions present minor influences. A series of empirical equations was developed to kinetically predict the dust-driven process. The Al-, Fe-, and Ti-bearing mineralogical components, as well as their mixtures, are thus recommended as appropriate proxies for the following laboratory research. The dust-driven heterogeneous γ values were calculated as 6.08×10^{-6} for dark reactions and 1.14×10^{-5} for photo-reactions, corresponding, respectively, to the atmospheric sulfate forma-

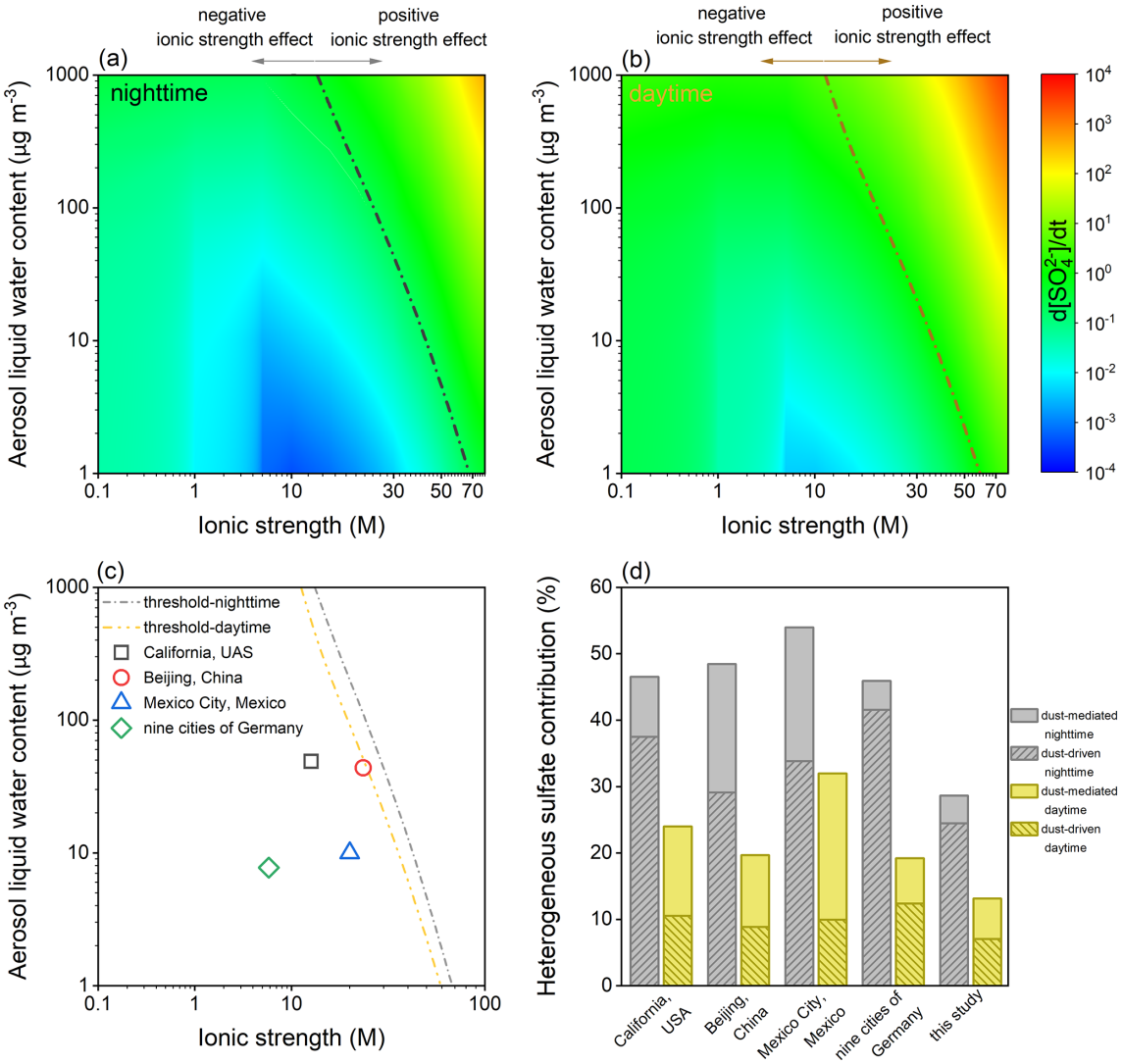

Figure 11. Joint influences of ionic strength (I) and aerosol liquid water content (ALWC) on the aqueous-phase oxidation of SO_2. Aqueous-phase sulfate formation rate varying with I and ALWC during **(a)** nighttime and **(b)** daytime. The dash-dotted lines indicate the thresholds distinguishing the negative and positive effects of ionic strength. **(c)** Reported I–ALWC relationships versus the nocturnal and diurnal thresholds. The field-observed data were collected from the measurements performed in California, USA (Stelson and Seinfeld, 1981), Beijing, China (Song et al., 2021), Mexico City, Mexico (Volkamer et al., 2007; Hennigan et al., 2015), and the nine cities of Germany (Scheinhardt et al., 2013). **(d)** Heterogeneous contribution proportions calculated by the reported I–ALWC relationships and parameterization of this study (ionic strength-free settings and an ALWC of 300 $\mu g\,m^{-3}$ for aqueous-phase oxidation; dust concentration of 55 $\mu g\,m^{-3}$ for heterogeneous oxidation).

tion rates of 0.195 and 0.365 $\mu g\,m^{-3}\,h^{-1}$ in the presence of 55 $\mu g\,m^{-3}$ of natural dust.

A comparison model was further developed to reveal the atmospheric relevance of the heterogeneous drivers for the dust surface. Dust heterogeneous oxidation is suggested to explain 28.6 % of the secondary sulfate aerosols during nighttime and 13.1 % during daytime, and the dust surface drivers act as the dominant contributors. Furthermore, dust heterogeneous oxidation affects the atmospheric lifetime of SO_2. The increased dust concentration may aggravate the secondary sulfate pollution and has the potential to explain the acknowledged missing sulfate formation rate (0.3–3.0 $\mu g\,m^{-3}\,h^{-1}$). The joint effects of I and ALWC on liquid kinetics influence the importance of the heterogeneous pathway. The heterogeneous contribution proportions estimated by the reported I–ALWC relationships are generally greater than those calculated by the parameterization in the current comparison model. Additionally, a dust heterogeneous pathway in the atmosphere is believed to be kinetically comparable with droplet interfacial oxidation.

Overall, this study suggests that the implementation of heterogeneous processes in atmospheric models will vastly im-

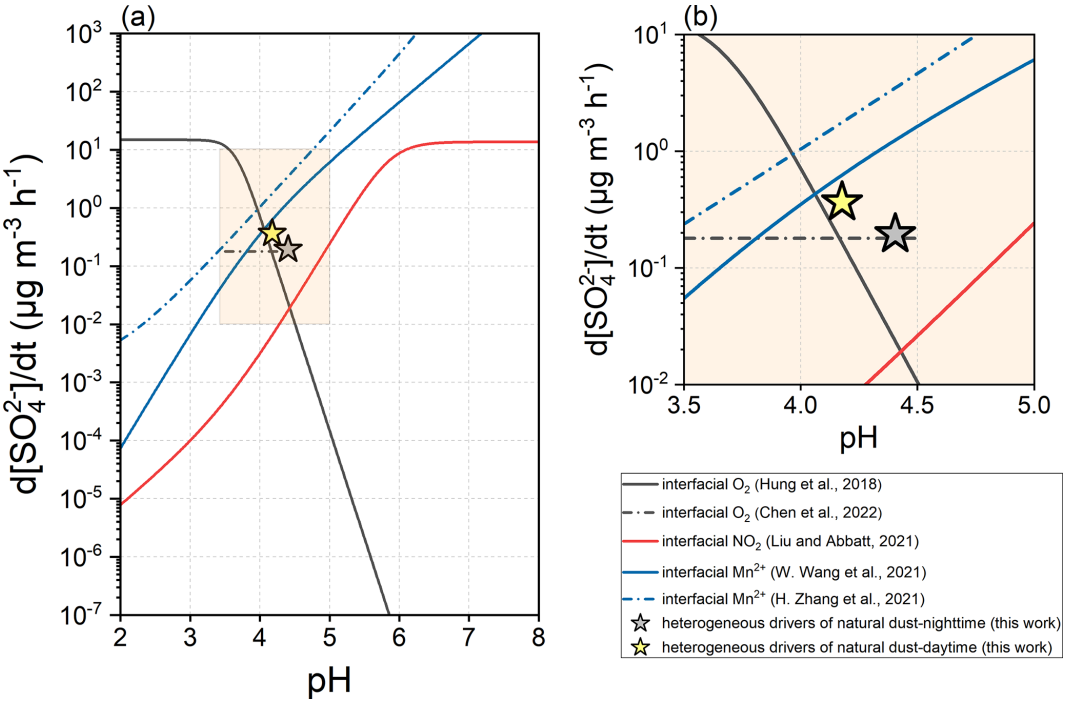

Figure 12. Kinetic comparison between microdroplet interfacial oxidation and the dust-driven heterogeneous pathway. The interfacial oxidation of SO_2 can be induced by the O_2, NO_2, or Mn^{2+} at aerosol particle interfaces. The O_2-dominated oxidation can be assessed by the method concluded by Hung et al. (2018). Chen et al. (2022) refreshed the assessment method relevant to interfacial O_2, and the result here was obtained under the ionic strength of 40 M within the pH range of 3.5–4.5. The NO_2-dominated oxidation was assessed based on the work of Liu and Abbatt (2021). The Mn^{2+}-dominated oxidation can be assessed by the methods of W. Wang et al. (2021) and H. Zhang et al. (2021). More parameterization and methodology details can be found in Text S5 of the Supplement.

prove the agreement between the modelled and observed sulfate concentrations. The dust heterogeneous pathway should be treated as a significant contributor of secondary sulfate. More necessarily, dust surface drivers are needed to be viewed as an important research focus. Zheng et al. (2015) revised the CMAQ model by adding a heterogeneous mechanism and observed the accurate simulation run upon determining the uptake coefficient to be 2.0×10^{-5}, which is higher than the γ values of the dust heterogeneous pathway herein (7.04×10^{-6} during nighttime and 1.55×10^{-5} during daytime). Hence, other solid aerosols, such as sea salts (Laskin et al., 2003; Rossi, 2003) and carbonaceous particles (He and He, 2020; F. Zhang et al., 2020), would better be taken into the following heterogeneous discussions together with the dust-related processes we studied.

Meteorological factors impact the atmospheric relevance of the dust heterogeneous pathway. Taking humidity as an example, on the dust surface, the heterogeneous reaction of SO_2 is humidity-dependent, and the exact dependence varies with the type of dust and the condition of the reaction (Huang et al., 2015; Park et al., 2017; Urupina et al., 2022). The uptake of gas-phase oxidants over the dust surface is also influenced by humidity (Kumar et al., 2014). For aerosol droplets, increased humidity elevates its liquid volume and radius (Wu et al., 2018; Ding et al., 2019). Aerosol liquid water serves as an efficient medium for multi-phase reactions (Wu et al., 2018; Yue et al., 2019), whereas the radius is negatively associated with the sulfate formation at the droplet interface (Hung et al., 2018; W. Wang et al., 2021; Chen et al., 2022). Furthermore, droplet acidity decreases as the liquid volume increases, thereby increasing the ionization of dissolved sulfur species, followed by the increased sulfate formation rate (Yue et al., 2019; Jin et al., 2020; Gao et al., 2022). Overall, how meteorological factors influence the relative importance of gas-phase, aqueous-phase, and heterogeneous pathways warrants further research.

Heterogeneous laboratory results were scarcely discussed together with other SO_2 conversion routes. This study attempted to set an example for kinetically comparing the heterogeneous oxidation characterized by laboratory work with the documented gas- and aqueous-phase data. Relative to the three-dimensional numerical models, the developed comparison model involves more oxidation pathways. Since the aqueous-phase oxidation here is relevant to aerosol droplets rather than cloud/fog droplets, the current parameterization could be more appropriate for simulating the fine particulate matter that was frequently collected by atmospheric observations and compared with modelling data. Furthermore, the

heterogeneous oxidation was classified into dust-mediated and dust-driven modes to better distinguish the key surface impactors. Therefore, this comparison model has advantages over the traditional atmospheric chemistry models and is recommended for the following heterogeneous laboratory research to systematically compare the experimental data with the acknowledged gas-phase, aqueous-phase, and heterogeneous oxidation pathways.

This work broadens the application of the infrared technique in atmospheric laboratory research. Apart from the uptake coefficient calculations normally concerned, this study moved forward to bridge the relationship between particle acidity and sulfate formation rate by analysing the shape and intensity of the infrared spectrum and further compared heterogeneous oxidation with other atmospheric pathways. This research not only provides a promising methodology for the future heterogeneous research utilizing the classic in situ DRIFTS approach, but also helps to take good advantage of the infrared technique in the laboratory studies in relation to atmospheric heterogeneous oxidation.

Data availability. A dataset for this paper can be accessed at https://data.mendeley.com/datasets/hyvdz7khs6/1 (Wang, 2022).

Supplement. The supplement related to this article is available online at: https://doi.org/10.5194/acp-22-13467-2022-supplement.

Author contributions. TW designed the experiments, processed the data, and wrote the paper together with YL. HC and ZW measured the physical and chemical properties of the particle samples. HF, JC, and LZ provided guidance on the data analysis and paper writing.

Competing interests. The contact author has declared that none of the authors has any competing interests.

Disclaimer. Publisher's note: Copernicus Publications remains neutral with regard to jurisdictional claims in published maps and institutional affiliations.

Financial support. This research has been supported by the National Natural Science Foundation of China (grant nos. 22176036, 21976030, 22006020, 42205099), the Natural Science Foundation of Shanghai (grant no. 19ZR1471200), and China Postdoctoral Science Foundation (grant no. 2021M700792).

Review statement. This paper was edited by Barbara Ervens and reviewed by three anonymous referees.

References

Abou-Ghanem, M., Oliynyk, A. O., Chen, Z., Matchett, L. C., McGrath, D. T., Katz, M. J., Locock, A. J., and Styler, S. A.: Significant Variability in the Photocatalytic Activity of Natural Titanium-Containing Minerals: Implications for Understanding and Predicting Atmospheric Mineral Dust Photochemistry, Environ. Sci. Technol., 54, 13509–13516, https://doi.org/10.1021/acs.est.0c05861, 2020.

Adams, J. W., Rodriguez, D., and Cox, R. A.: The uptake of SO_2 on Saharan dust: a flow tube study, Atmos. Chem. Phys., 5, 2679–2689, https://doi.org/10.5194/acp-5-2679-2005, 2005.

Alexander, B., Park, R. J., Jacob, D. J., and Gong, S.: Transition metal-catalyzed oxidation of atmospheric sulfur: Global implications for the sulfur budget, J. Geophys. Res., 114, D2309, https://doi.org/10.1029/2008JD010486, 2009.

Alexander, B., Allman, D. J., Amos, H. M., Fairlie, T. D., Dachs, J., Hegg, D. A., and Sletten, R. S.: Isotopic constraints on the formation pathways of sulfate aerosol in the marine boundary layer of the subtropical northeast Atlantic Ocean, J. Geophys. Res.-Atmos., 117, D6304, https://doi.org/10.1029/2011JD016773, 2012.

Antoniou, M. G., Boraei, I., Solakidou, M., Deligiannakis, Y., Abhishek, M., Lawton, L. A., and Edwards, C.: Enhancing photocatalytic degradation of the cyanotoxin microcystin-LR with the addition of sulfate-radical generating oxidants, J. Hazard. Mater., 360, 461–470, https://doi.org/10.1016/j.jhazmat.2018.07.111, 2018.

Ault, A. P.: Aerosol Acidity: Novel Measurements and Implications for Atmospheric Chemistry, Accounts Chem. Res., 53, 1703–1714, https://doi.org/10.1021/acs.accounts.0c00303, 2020.

Baltrusaitis, J., Cwiertny, D. M., and Grassian, V. H.: Adsorption of sulfur dioxide on hematite and goethite particle surfaces, Phys. Chem. Chem. Phys., 9, 5542–5554, https://doi.org/10.1039/b709167b, 2007.

Baltrusaitis, J., Jayaweera, P. M., and Grassian, V. H.: Sulfur Dioxide Adsorption on TiO_2 Nanoparticles: Influence of Particle Size, Coadsorbates, Sample Pretreatment, and Light on Surface Speciation and Surface Coverage, J. Phys. Chem. C, 115, 492–500, https://doi.org/10.1021/jp108759b, 2010.

Berglen, T. F., Berntsen, T. K., Isaksen, I. S. A., and Sundet, J. K.: A global model of the coupled sulfur/oxidant chemistry in the troposphere: The sulfur cycle, J. Geophys. Res., 109, D19310, https://doi.org/10.1029/2003JD003948, 2004.

Bian, H. and Zender, C. S.: Mineral dust and global tropospheric chemistry: Relative roles of photolysis and heterogeneous uptake, J. Geophys. Res.-Atmos., 108, 4672, https://doi.org/10.1029/2002JD003143, 2003.

Chen, H., Nanayakkara, C. E., and Grassian, V. H.: Titanium dioxide photocatalysis in atmospheric chemistry, Chem. Rev., 112, 5919–5948, https://doi.org/10.1021/cr3002092, 2012.

Chen, Q., Schmidt, J. A., Shah, V., Jaeglé, L., Sherwen, T., and Alexander, B.: Sulfate production by reactive bromine: Implications for the global sulfur and reactive bromine budgets, Geophys. Res. Lett., 44, 7069–7078, https://doi.org/10.1002/2017GL073812, 2017.

Chen, Y., Tong, S., Li, W., Liu, Y., Tan, F., Ge, M., Xie, X., and Sun, J.: Photocatalytic Oxidation of SO_2 by TiO_2: Aerosol Formation and the Key Role of Gaseous Reac-

tive Oxygen Species, Environ. Sci. Technol., 55, 9784–9793, https://doi.org/10.1021/acs.est.1c01608, 2021.

Chen, Z., Liu, P., Wang, W., Cao, X., Liu, Y., Zhang, Y., and Ge, M.: Rapid Sulfate Formation via Uncatalyzed Autoxidation of Sulfur Dioxide in Aerosol Microdroplets, Environ. Sci. Technol., 56, 7637–7646, https://doi.org/10.1021/acs.est.2c00112, 2022.

Cheng, Y., Zheng, G., Wei, C., Mu, Q., Zheng, B., Wang, Z., Gao, M., Zhang, Q., He, K., Carmichael, G., Pöschl, U., and Su, H.: Reactive nitrogen chemistry in aerosol water as a source of sulfate during haze events in China, Sci. Adv., 2, e1601530, https://doi.org/10.1126/sciadv.1601530, 2016.

Chu, B., Wang, Y., Yang, W., Ma, J., Ma, Q., Zhang, P., Liu, Y., and He, H.: Effects of NO_2 and C_3H_6 on the heterogeneous oxidation of SO_2 on TiO_2 in the presence or absence of UV–Vis irradiation, Atmos. Chem. Phys., 19, 14777–14790, https://doi.org/10.5194/acp-19-14777-2019, 2019.

Chughtai, A. R., Brooks, M. E., and Smith, D. M.: Effect of metal oxides and black carbon (soot) on SO_2 / O_2 / H_2O reaction systems, Aerosol Sci. Tech., 19, 121–132, https://doi.org/10.1080/02786829308959626, 1993.

Clegg, M. and Abbatt, D.: Uptake of Gas-Phase SO_2 and H_2O_2 by Ice Surfaces: Dependence on Partial Pressure, Temperature, and Surface Acidity, J. Phys. Chem. A, 105, 6630–6636, https://doi.org/10.1021/jp010062r, 2001a.

Clegg, S. M. and Abbatt, J. P. D.: Oxidation of SO_2 by H_2O_2 on ice surfaces at 228 K: a sink for SO_2 in ice clouds, Atmos. Chem. Phys., 1, 73–78, https://doi.org/10.5194/acp-1-73-2001, 2001b.

Darif, B., Ojala, S., Pirault-Roy, L., Bensitel, M., Brahmi, R., and Keiski, R. L.: Study on the catalytic oxidation of DMDS over Pt-Cu catalysts supported on Al_2O_3, $AlSi_{20}$ and SiO_2, Appl. Catal. B, 181, 24–33, https://doi.org/10.1016/j.apcatb.2015.07.050, 2016.

Davidovits, P., Kolb, C. E., Williams, L. R., Jayne, J. T., and Worsnop, D. R.: Mass Accommodation and Chemical Reactions at Gas-Liquid Interfaces, Chem. Rev., 106, 1323–1354, https://doi.org/10.1021/cr040366k, 2006.

Ding, J., Zhao, P., Su, J., Dong, Q., Du, X., and Zhang, Y.: Aerosol pH and its driving factors in Beijing, Atmos. Chem. Phys., 19, 7939–7954, https://doi.org/10.5194/acp-19-7939-2019, 2019.

Du, C., Kong, L., Zhanzakova, A., Tong, S., Yang, X., Wang, L., Fu, H., Cheng, T., Chen, J., and Zhang, S.: Impact of adsorbed nitrate on the heterogeneous conversion of SO_2 on α-Fe_2O_3 in the absence and presence of simulated solar irradiation, Sci. Total Environ., 649, 1393–1402, https://doi.org/10.1016/j.scitotenv.2018.08.295, 2019.

Dupart, Y., King, S. M., Nekat, B., Nowak, A., Wiedensohler, A., Herrmann, H., David, G., Thomas, B., Miffre, A., Rairoux, P., Anna, B. D., and George, C.: Mineral dust photochemistry induces nucleation events in the presence of SO_2, P. Natl. Acad. Sci. USA, 109, 20842–20847, https://doi.org/10.1073/pnas.1212297109, 2012.

Fairlie, T. D., Jacob, D. J., Dibb, J. E., Alexander, B., Avery, M. A., van Donkelaar, A., and Zhang, L.: Impact of mineral dust on nitrate, sulfate, and ozone in transpacific Asian pollution plumes, Atmos. Chem. Phys., 10, 3999–4012, https://doi.org/10.5194/acp-10-3999-2010, 2010.

Fan, M., Zhang, Y., Lin, Y., Li, J., Cheng, H., An, N., Sun, Y., Qiu, Y., Cao, F., and Fu, P.: Roles of Sulfur Oxidation Pathways in the Variability in Stable Sulfur Isotopic Composition of Sulfate Aerosols at an Urban Site in Beijing, China, Environ. Sci. Technol. Lett., 7, 883–888, https://doi.org/10.1021/acs.estlett.0c00623, 2020.

Filonchyk, M.: Characteristics of the severe March 2021 Gobi Desert dust storm and its impact on air pollution in China, Chemosphere, 287, 132219, https://doi.org/10.1016/j.chemosphere.2021.132219, 2022.

Fu, H., Cwiertny, D. M., Carmichael, G. R., Scherer, M. M., and Grassian, V. H.: Photoreductive dissolution of Fe-containing mineral dust particles in acidic media, J. Geophys. Res., 115, D11304, https://doi.org/10.1029/2009JD012702, 2010.

Fu, H., Wang, X., Wu, H., Yin, Y., and Chen, J.: Heterogeneous uptake and oxidation of SO_2 on iron oxides, J. Phys. Chem. C, 111, 6077–6085, https://doi.org/10.1021/jp070087b, 2007.

Fu, H., Xu, T., Yang, S., Zhang, S., and Chen, J.: Photoinduced formation of Fe(III)-sulfato complexes on the surface of α-Fe_2O_3 and their photochemical performance, J. Phys. Chem. C, 113, 11316–11322, https://doi.org/10.1021/jp8088275, 2009.

Gao, J., Shi, G., Zhang, Z., Wei, Y., Tian, X., Feng, Y., Russell, A. G., and Nenes, A.: Targeting Atmospheric Oxidants Can Better Reduce Sulfate Aerosol in China: H_2O_2 Aqueous Oxidation Pathway Dominates Sulfate Formation in Haze, Environ. Sci. Technol., 56, 10608–10618, https://doi.org/10.1021/acs.est.2c01739, 2022.

Gaston, C. J., Pratt, K. A., Suski, K. J., May, N. W., Gill, T. E., and Prather, K. A.: Laboratory Studies of the Cloud Droplet Activation Properties and Corresponding Chemistry of Saline Playa Dust, Environ. Sci. Technol., 51, 1348–1356, https://doi.org/10.1021/acs.est.6b04487, 2017.

Gen, M., Zhang, R., Huang, D., Li, Y., and Chan, C. K.: Heterogeneous Oxidation of SO_2 in Sulfate Production during Nitrate Photolysis at 300 nm: Effect of pH, Relative Humidity, Irradiation Intensity, and the Presence of Organic Compounds, Environ. Sci. Technol., 53, 8757–8766, https://doi.org/10.1021/acs.est.9b01623, 2019.

Goodman, A. L., Li, P., Usher, C. R., and Grassian, V. H.: Heterogeneous uptake of sulfur dioxide on aluminum and magnesium oxide particles, J. Phys. Chem. A, 105, 6109–6120, https://doi.org/10.1021/jp004423z, 2001.

Guan, C., Li, X., Luo, Y., and Huang, Z.: Heterogeneous Reaction of NO_2 on α-Al_2O_3 in the Dark and Simulated Sunlight, J. Phys. Chem. A, 118, 6999–7006, https://doi.org/10.1021/jp503017k, 2014.

Han, L., Liu, X., Chen, Y., Xiang, X., Cheng, S., and Wang, H.: Key factors influencing the formation of sulfate aerosol on the surface of mineral aerosols: Insights from laboratory simulations and ACSM measurements, Atmos. Environ., 253, 118341, https://doi.org/10.1016/j.atmosenv.2021.118341, 2021.

Hanson, D. R., Ravishankara, A. R., and Solomon, S.: Heterogeneous reactions in sulfuric acid aerosols: A framework for model calculations, J. Geophys. Res.-Atmos., 99, 3615–3629, https://doi.org/10.1029/93JD02932, 1994.

Harris, E., Sinha, B., Foley, S., Crowley, J. N., Borrmann, S., and Hoppe, P.: Sulfur isotope fractionation during heterogeneous oxidation of SO_2 on mineral dust, Atmos. Chem. Phys., 12, 4867–4884, https://doi.org/10.5194/acp-12-4867-2012, 2012.

Haynes, W. M.: Handbook of Chemistry and Physics, CRC Press, New York, ISBN 084930458X, 2014.

He, G. and He, H.: Water Promotes the Oxidation of SO_2 by O_2 over Carbonaceous Aerosols, Environ. Sci. Technol., 54, 7070–7077, https://doi.org/10.1021/acs.est.0c00021, 2020.

He, H., Wang, Y., Ma, Q., Ma, J., Chu, B., Ji, D., Tang, G., Liu, C., Zhang, H., and Hao, J.: Mineral dust and NO_x promote the conversion of SO_2 to sulfate in heavy pollution days, Sci. Rep.-UK, 4, 4172, https://doi.org/10.1038/srep04172, 2014.

He, P., Alexander, B., Geng, L., Chi, X., Fan, S., Zhan, H., Kang, H., Zheng, G., Cheng, Y., Su, H., Liu, C., and Xie, Z.: Isotopic constraints on heterogeneous sulfate production in Beijing haze, Atmos. Chem. Phys., 18, 5515–5528, https://doi.org/10.5194/acp-18-5515-2018, 2018.

He, X. and Zhang, Y.: Influence of relative humidity on SO_2 oxidation by O_3 and NO_2 on the surface of TiO_2 particles: Potential for formation of secondary sulfate aerosol, Spectrochim. Acta Pt. A, 219, 121–128, https://doi.org/10.1016/j.saa.2019.04.046, 2019.

Hennigan, C. J., Izumi, J., Sullivan, A. P., Weber, R. J., and Nenes, A.: A critical evaluation of proxy methods used to estimate the acidity of atmospheric particles, Atmos. Chem. Phys., 15, 2775–2790, https://doi.org/10.5194/acp-15-2775-2015, 2015.

Himmelblau, D. M.: Diffusion of dissolved gases in liquids, Chem. Rev., 64, 527–550, https://doi.org/10.1021/cr60231a002, 1964.

Huang, L., Zhao, Y., Li, H., and Chen, Z.: Kinetics of heterogeneous reaction of sulfur dioxide on authentic mineral dust: effects of relative humidity and hydrogen peroxide, Environ. Sci. Technol., 49, 10797–10805, https://doi.org/10.1021/acs.est.5b03930, 2015.

Huang, L., Zhao, Y., Li, H., and Chen, Z.: Hydrogen peroxide maintains the heterogeneous reaction of sulfur dioxide on mineral dust proxy particles, Atmos. Environ., 141, 552–559, https://doi.org/10.1016/j.atmosenv.2016.07.035, 2016.

Huang, L., An, J., Koo, B., Yarwood, G., Yan, R., Wang, Y., Huang, C., and Li, L.: Sulfate formation during heavy winter haze events and the potential contribution from heterogeneous $SO_2 + NO_2$ reactions in the Yangtze River Delta region, China, Atmos. Chem. Phys., 19, 14311–14328, https://doi.org/10.5194/acp-19-14311-2019, 2019.

Huang, Z., Zhang, Z., Kong, W., Feng, S., Qiu, Y., Tang, S., Xia, C., Ma, L., Luo, M., and Xu, D.: Synergistic effect among Cl_2, SO_2 and NO_2 in their heterogeneous reactions on gamma-alumina, Atmos. Environ., 166, 403–411, https://doi.org/10.1016/j.atmosenv.2017.06.041, 2017.

Hung, H. and Hoffmann, M. R.: Oxidation of Gas-Phase SO_2 on the Surfaces of Acidic Microdroplets: Implications for Sulfate and Sulfate Radical Anion Formation in the Atmospheric Liquid Phase, Environ. Sci. Technol., 49, 13768–13776, https://doi.org/10.1021/acs.est.5b01658, 2015.

Hung, H., Hsu, M., and Hoffmann, M. R.: Quantification of SO_2 Oxidation on Interfacial Surfaces of Acidic Micro-Droplets: Implication for Ambient Sulfate Formation, Environ. Sci. Technol., 52, 9079–9086, https://doi.org/10.1021/acs.est.8b01391, 2018.

Jacob, D. J.: Heterogeneous chemistry and tropospheric ozone, Atmos. Environ., 34, 2131–2159, https://doi.org/10.1016/S1352-2310(99)00462-8, 2000.

Jayne, J. T. and Davidovits, P.: Uptake of SO_2(g) by Aqueous Surfaces as a Function of pH: The Effect of Chemical Reaction at the Interface, J. Phys. Chem., 94, 6041–6048, https://doi.org/10.1021/j100378a076, 1990.

Jin, X., Wang, Y., Li, Z., Zhang, F., Xu, W., Sun, Y., Fan, X., Chen, G., Wu, H., Ren, J., Wang, Q., and Cribb, M.: Significant contribution of organics to aerosol liquid water content in winter in Beijing, China, Atmos. Chem. Phys., 20, 901–914, https://doi.org/10.5194/acp-20-901-2020, 2020.

Ke, Z., Liu, X., Wu, M., Shan, Y., and Shi, Y.: Improved Dust Representation and Impacts on Dust Transport and Radiative Effect in CAM5, J. Adv. Model. Earth Sy., 14, e2021MS002845, https://doi.org/10.1029/2021MS002845, 2022.

Keene, W. C., Pszenny, A. A. P., Maben, J. R., Stevenson, E., and Wall, A.: Closure evaluation of size-resolved aerosol pH in the New England coastal atmosphere during summer, J. Geophys. Res.-Atmos., 109, D23307, https://doi.org/10.1029/2004JD004801, 2004.

Kim, J., Choe, Y. J., Kim, S. H., and Jeong, K.: Enhancing the decomposition of refractory contaminants on SO_4^{2-}-functionalized iron oxide to accommodate surface $SO_4^{\bullet}$-generated via radical transfer from $^{\bullet}OH$, Appl. Catal. B, 252, 62–76, https://doi.org/10.1016/j.apcatb.2019.04.015, 2019.

Kong, L. D., Zhao, X., Sun, Z. Y., Yang, Y. W., Fu, H. B., Zhang, S. C., Cheng, T. T., Yang, X., Wang, L., and Chen, J. M.: The effect of nitrate on the heterogeneous uptake of sulfur dioxide on hematite, Atmos. Chem. Phys., 14, 9451–9467, https://doi.org/10.5194/acp-14-9451-2014, 2014.

Kumar, R., Barth, M. C., Madronich, S., Naja, M., Carmichael, G. R., Pfister, G. G., Knote, C., Brasseur, G. P., Ojha, N., and Sarangi, T.: Effects of dust aerosols on tropospheric chemistry during a typical pre-monsoon season dust storm in northern India, Atmos. Chem. Phys., 14, 6813–6834, https://doi.org/10.5194/acp-14-6813-2014, 2014.

Laskin, A., Gaspar, D. J., Wang, W., Hunt, S. W., Cowin, J. P., Colson, S. D., and Finlayson-Pitts, B. J.: Reactions at Interfaces as a Source of Sulfate Formation in Sea-Salt Particles, Science, 301, 340–344, https://doi.org/10.1126/science.1085374, 2003.

Li, G., Bei, N., Cao, J., Huang, R., and Wu, J.: A possible pathway for rapid growth of sulfate during haze days in China, Atmos. Chem. Phys., 17, 3301–3316, https://doi.org/10.5194/acp-17-3301-2017, 2017.

Li, G., Lu, D., Yang, X., Zhang, H., Guo, Y., Qu, G., Wang, P., Chen, L., Ruan, T., Hou, X., Jin, X., Zhang, R., Tan, Q., Zhai, S., Ma, Y., Yang, R., Fu, J., Shi, J., Liu, G., Wang, Q., Liang, Y., Zhang, Q., Liu, Q., and Jiang, G.: Resurgence of Sandstorms Complicates China's Air Pollution Situation, Environ. Sci. Technol., 55, 11467–11469, https://doi.org/10.1021/acs.est.1c03724, 2021.

Li, J., Shang, J., and Zhu, T.: Heterogeneous reactions of SO_2 on ZnO particle surfaces, Sci. China: Chem., 54, 161–166, https://doi.org/10.1007/s11426-010-4167-9, 2010.

Li, J., Zhang, Y., Cao, F., Zhang, W., Fan, M., Lee, X., and Michalski, G.: Stable Sulfur Isotopes Revealed a Major Role of Transition-Metal Ion-Catalyzed SO_2 Oxidation in Haze Episodes, Environ. Sci. Technol., 54, 2626–2634, https://doi.org/10.1021/acs.est.9b07150, 2020.

Li, K., Fang, X., Wang, T., Gong, K., Ali Tahir, M., Wang, W., Han, J., Cheng, H., Xu, G., and Zhang, L.: Atmospheric organic complexation enhanced sulfate formation and iron dissolution on nano α-Fe_2O_3, Environ. Sci. Nano, 8, 698–710, https://doi.org/10.1039/D0EN01220C, 2021.

Li, K., Kong, L., Zhanzakova, A., Tong, S., Shen, J., Wang, T., Chen, L., Li, Q., Fu, H., and Zhang, L.: Heterogeneous Con-

version of SO_2 on Nano α-Fe_2O_3: the Effect of Morphology, Light Illumination and Relative Humidity, Environ. Sci. Nano, 6, 1838–1851, https://doi.org/10.1039/C9EN00097F, 2019.

Li, L., Chen, Z. M., Zhang, Y. H., Zhu, T., Li, J. L., and Ding, J.: Kinetics and mechanism of heterogeneous oxidation of sulfur dioxide by ozone on surface of calcium carbonate, Atmos. Chem. Phys., 6, 2453–2464, https://doi.org/10.5194/acp-6-2453-2006, 2006.

Li, L., Chen, Z. M., Zhang, Y. H., Zhu, T., Li, S., Li, H. J., Zhu, L. H., and Xu, B. Y.: Heterogeneous oxidation of sulfur dioxide by ozone on the surface of sodium chloride and its mixtures with other components, J. Geophys. Res., 112, D18301, https://doi.org/10.1029/2006JD008207, 2007.

Li, T., Wang, X., Chen, Y., Liang, J., and Zhou, L.: Producing $^{\bullet}OH$, $SO_4^{\bullet-}$ and $^{\bullet}O_2^-$ in heterogeneous Fenton reaction induced by Fe_3O_4-modified schwertmannite, Chem. Eng. J., 393, 124735, https://doi.org/10.1016/j.cej.2020.124735, 2020.

Li, S., Zhang, F., Jin, X., Sun, Y., Wu, H., Xie, C., Chen, L., Liu, J., Wu, T., Jiang, S., Cribb, M., and Li, Z.: Characterizing the ratio of nitrate to sulfate in ambient fine particles of urban Beijing during 2018–2019, Atmos. Environ., 237, 117662, https://doi.org/10.1016/j.atmosenv.2020.117662, 2020.

Lind, J. A., Lazrus, A. L., and Kok, G. L.: Aqueous phase oxidation of sulfur(IV) by hydrogen peroxide, methylhydroperoxide, and peroxyacetic acid, J. Geophys. Res., 92, 4171–4177, https://doi.org/10.1029/JD092iD04p04171, 1987.

Liu, C., Ma, Q., Liu, Y., Ma, J., and He, H.: Synergistic reaction between SO_2 and NO_2 on mineral oxides: a potential formation pathway of sulfate aerosol, Phys. Chem. Chem. Phys., 14, 1668–1676, https://doi.org/10.1039/C1CP22217A, 2012.

Liu, J., Wu, D., Fan, S., Mao, X., and Chen, H.: A one-year, on-line, multi-site observational study on water-soluble inorganic ions in $PM_{2.5}$ over the Pearl River Delta region, China, Sci. Total Environ., 601/602, 1720–1732, https://doi.org/10.1016/j.scitotenv.2017.06.039, 2017.

Liu, T. and Abbatt, J. P. D.: Oxidation of sulfur dioxide by nitrogen dioxide accelerated at the interface of deliquesced aerosol particles, Nat. Chem., 13, 1173–1177, https://doi.org/10.1038/s41557-021-00777-0, 2021.

Liu, T., Clegg, S. L., and Abbatt, J. P. D.: Fast oxidation of sulfur dioxide by hydrogen peroxide in deliquesced aerosol particles, P. Natl. Acad. Sci. USA, 117, 1354–1359, https://doi.org/10.1073/pnas.1916401117, 2020.

Liu, T., Chan, A. W. H., and Abbatt, J. P. D.: Multiphase Oxidation of Sulfur Dioxide in Aerosol Particles: Implications for Sulfate Formation in Polluted Environments, Environ. Sci. Technol., 55, 4227–4242, https://doi.org/10.1021/acs.est.0c06496, 2021.

Liu, W., He, X., Pang, S., and Zhang, Y.: Effect of relative humidity on O_3 and NO_2 oxidation of SO_2 on α-Al_2O_3 particles, Atmos. Environ., 167, 245–253, https://doi.org/10.1016/j.atmosenv.2017.08.028, 2017.

Liu, X., Chen, W., and Jiang, H.: Facile synthesis of Ag / Ag_3PO_4 / AMB composite with improved photocatalytic performance, Chem. Eng. J., 308, 889–896, https://doi.org/10.1016/j.cej.2016.09.125, 2017.

Liu, Y., Wang, T., Fang, X., Deng, Y., Cheng, H., Fu, H., and Zhang, L.: Impact of greenhouse gas CO_2 on the heterogeneous reaction of SO_2 on alpha-Al_2O_3, Chinese Chem. Lett., 31, 2712–2716, https://doi.org/10.1016/j.cclet.2020.04.037, 2020.

Liu, Y., Feng, Z., Zheng, F., Bao, X., Liu, P., Ge, Y., Zhao, Y., Jiang, T., Liao, Y., Zhang, Y., Fan, X., Yan, C., Chu, B., Wang, Y., Du, W., Cai, J., Bianchi, F., Petäjä, T., Mu, Y., He, H., and Kulmala, M.: Ammonium nitrate promotes sulfate formation through uptake kinetic regime, Atmos. Chem. Phys., 21, 13269–13286, https://doi.org/10.5194/acp-21-13269-2021, 2021.

Liu, Y., Deng, Y., Liu, J., Fang, X., Wang, T., Li, K., Gong, K., Bacha, A. U., Nabi, I., Ge, Q., Zhang, X., George, C., and Zhang, L.: A novel pathway of atmospheric sulfate formation through carbonate radicals, Atmos. Chem. Phys., 22, 9175–9197, https://doi.org/10.5194/acp-22-9175-2022, 2022.

Ma, Q., Liu, Y., and He, H.: Synergistic effect between NO_2 and SO_2 in their adsorption and reaction on γ-Alumina, J. Phys. Chem. A, 112, 6630–6635, https://doi.org/10.1021/jp802025z, 2008.

Ma, Q., Liu, Y., Liu, C., Ma, J., and He, H.: A case study of Asian dust storm particles: Chemical composition, reactivity to SO_2 and hygroscopic properties, J. Environ. Sci., 24, 62–71, https://doi.org/10.1016/S1001-0742(11)60729-8, 2012.

Ma, Q., Wang, T., Liu, C., He, H., Wang, Z., Wang, W., and Liang, Y.: SO_2 initiates the efficient conversion of NO_2 to HONO on MgO surface, Environ. Sci. Technol., 51, 3767–3775, https://doi.org/10.1021/acs.est.6b05724, 2017.

Ma, Q., Wang, L., Chu, B., Ma, J., and He, H.: Contrary Role of H_2O and O_2 in the Kinetics of Heterogeneous Photochemical Reactions of SO_2 on TiO_2, J. Phys. Chem. A, 123, 1311–1318, https://doi.org/10.1021/acs.jpca.8b11433, 2018.

Martin, M. A., Childers, J. W., and Palmer, R. A.: Fourier transform infrared photoacoustic spectroscopy characterization of sulfur-oxygen species resulting from the reaction of SO_2 with CaO and $CaCO_3$, Appl. Spectrosc., 41, 120–126, https://doi.org/10.1366/0003702874868151, 1987.

Maters, E. C., Delmelle, P., Rossi, M. J., and Ayris, P. M.: Reactive Uptake of Sulfur Dioxide and Ozone on Volcanic Glass and Ash at Ambient Temperature, J. Geophys. Res.-Atmos., 122, 10077–10088, https://doi.org/10.1002/2017JD026993, 2017.

Mauldin III, R. L., Berndt, T., Sipilä, M., Paasonen, P., Petäjä, T., Kim, S., Kurtén, T., Stratmann, F., Kerminen, V. M., and Kulmala, M.: A new atmospherically relevant oxidant of sulphur dioxide, Nature, 488, 193–196, https://doi.org/10.1038/nature11278, 2012.

Nanayakkara, C. E., Pettibone, J., and Grassian, V. H.: Sulfur dioxide adsorption and photooxidation on isotopically-labeled titanium dioxide nanoparticle surfaces: roles of surface hydroxyl groups and adsorbed water in the formation and stability of adsorbed sulfite and sulfate, Phys. Chem. Chem. Phys., 14, 6957–6966, https://doi.org/10.1039/c2cp23684b, 2012.

Nanayakkara, C. E., Larish, W. A., and Grassian, V. H.: Titanium dioxide nanoparticle surface reactivity with atmospheric gases, CO_2, SO_2, and NO_2: roles of surface hydroxyl groups and adsorbed water in the formation and stability of adsorbed products, J. Phys. Chem. C, 118, 23011–23021, https://doi.org/10.1021/jp504402z, 2014.

Ndour, M., Nicolas, M., D'Anna, B., Ka, O., and George, C.: Photoreactivity of NO_2 on mineral dusts originating from different locations of the Sahara desert, Phys. Chem. Chem. Phys., 11, 1312–1319, https://doi.org/10.1039/b806441e, 2009.

Park, J. and Jang, M.: Heterogeneous photooxidation of sulfur dioxide in the presence of airborne mineral dust particles, RSC Adv., 6, 58617–58627, https://doi.org/10.1039/C6RA09601H, 2016.

Park, J., Ivanov, A. V., and Molina, M. J.: Effect of Relative Humidity on OH Uptake by Surfaces of Atmospheric Importance, J. Phys. Chem. A, 112, 6968–6977, https://doi.org/10.1021/jp8012317, 2008.

Park, J., Jang, M., and Yu, Z.: Heterogeneous Photo-oxidation of SO_2 in the Presence of Two Different Mineral Dust Particles: Gobi and Arizona Dust, Environ. Sci. Technol., 51, 9605–9613, https://doi.org/10.1021/acs.est.7b00588, 2017.

Peak, D., Ford, R. G., and Sparks, D. L.: An in situ ATR-FTIR investigation of sulfate bonding mechanisms on Goethite., J. Colloid Interf. Sci., 218, 289–299, https://doi.org/10.1006/jcis.1999.6405, 1999.

Persson, P. and Vgren, L. L.: Potentiometric and spectroscopic studies of sulfate complexation at the goethite-water interface, Geochim. Cosmochim. Ac., 60, 2789–2799, https://doi.org/10.1016/0016-7037(96)00124-X, 1996.

Pye, H. O. T., Nenes, A., Alexander, B., Ault, A. P., Barth, M. C., Clegg, S. L., Collett Jr., J. L., Fahey, K. M., Hennigan, C. J., Herrmann, H., Kanakidou, M., Kelly, J. T., Ku, I., McNeill, V. F., Riemer, N., Schaefer, T., Shi, G., Tilgner, A., Walker, J. T., Wang, T., Weber, R., Xing, J., Zaveri, R. A., and Zuend, A.: The acidity of atmospheric particles and clouds, Atmos. Chem. Phys., 20, 4809–4888, https://doi.org/10.5194/acp-20-4809-2020, 2020.

Ravishankara, A. R.: Heterogeneous and Multiphase Chemistry in the Troposphere, Science, 276, 1058–1064, https://doi.org/10.1126/science.276.5315.1058, 1997.

Ren, Y., Wei, J., Wu, Z., Ji, Y., Bi, F., Gao, R., Wang, X., Wang, G., and Li, H.: Chemical components and source identification of $PM_{2.5}$ in non-heating season in Beijing: The influences of biomass burning and dust, Atmos. Res., 251, 105412, https://doi.org/10.1016/j.atmosres.2020.105412, 2021.

Rindelaub, J. D., Craig, R. L., Nandy, L., Bondy, A. L., Dutcher, C. S., Shepson, P. B., and Ault, A. P.: Direct Measurement of pH in Individual Particles via Raman Microspectroscopy and Variation in Acidity with Relative Humidity, J. Phys. Chem. A, 120, 911–917, https://doi.org/10.1021/acs.jpca.5b12699, 2016.

Rossi, M. J.: Heterogeneous Reactions on Salts, Chem. Rev., 103, 4823–4882, https://doi.org/10.1021/cr020507n, 2003.

Rubasinghege, G. and Grassian, V. H.: Role(s) of adsorbed water in the surface chemistry of environmental interfaces, Chem. Commun., 49, 3071–3094, https://doi.org/10.1039/C3CC38872G, 2013.

Sakata, K., Takahashi, Y., Takano, S., Matsuki, A., Sakaguchi, A., and Tanimoto, H.: First X-ray Spectroscopic Observations of Atmospheric Titanium Species: Size Dependence and the Emission Source, Environ. Sci. Technol., 55, 10975–10986, https://doi.org/10.1021/acs.est.1c02000, 2021.

Sarwar, G., Fahey, K., Kwok, R., Gilliam, R. C., Roselle, S. J., Mathur, R., Xue, J., Yu, J., and Carter, W. P. L.: Potential impacts of two SO_2 oxidation pathways on regional sulfate concentrations: Aqueous-phase oxidation by NO_2 and gas-phase oxidation by Stabilized Criegee Intermediates, Atmos. Environ., 68, 186–197, https://doi.org/10.1016/j.atmosenv.2012.11.036, 2013.

Scheinhardt, S., Müller, K., Spindler, G., and Herrmann, H.: Complexation of trace metals in size-segregated aerosol particles at nine sites in Germany, Atmos. Environ., 74, 102–109, https://doi.org/10.1016/j.atmosenv.2013.03.023, 2013.

Seinfeld, J. and Pandis, S.: Atmospheric Chemistry and Physics: From Air Pollution to Climate Change, 3rd Edn., Wiley, ISBN 978-1-118-94740-1, 2016.

Shang, J., Li, J., and Zhu, T.: Heterogeneous reaction of SO_2 on TiO_2 particles, Sci. China Chem., 53, 2637–2643, https://doi.org/10.1007/s11426-010-4160-3, 2010.

Shao, J., Chen, Q., Wang, Y., Lu, X., He, P., Sun, Y., Shah, V., Martin, R. V., Philip, S., Song, S., Zhao, Y., Xie, Z., Zhang, L., and Alexander, B.: Heterogeneous sulfate aerosol formation mechanisms during wintertime Chinese haze events: air quality model assessment using observations of sulfate oxygen isotopes in Beijing, Atmos. Chem. Phys., 19, 6107–6123, https://doi.org/10.5194/acp-19-6107-2019, 2019.

Shi, Z., Krom, M. D., Jickells, T. D., Bonneville, S., Carslaw, K. S., Mihalopoulos, N., Baker, A. R., and Benning, L. G.: Impacts on iron solubility in the mineral dust by processes in the source region and the atmosphere: A review, Aeolian Res., 5, 21–42, https://doi.org/10.1016/j.aeolia.2012.03.001, 2012.

Song, S., Nenes, A., Gao, M., Zhang, Y., Liu, P., Shao, J., Ye, D., Xu, W., Lei, L., Sun, Y., Liu, B., Wang, S., and McElroy, M. B.: Thermodynamic Modeling Suggests Declines in Water Uptake and Acidity of Inorganic Aerosols in Beijing Winter Haze Events during 2014/2015–2018/2019, Environ. Sci. Technol. Lett., 6, 752–760, https://doi.org/10.1021/acs.estlett.9b00621, 2019.

Song, H., Lu, K., Ye, C., Dong, H., Li, S., Chen, S., Wu, Z., Zheng, M., Zeng, L., Hu, M., and Zhang, Y.: A comprehensive observation-based multiphase chemical model analysis of sulfur dioxide oxidations in both summer and winter, Atmos. Chem. Phys., 21, 13713–13727, https://doi.org/10.5194/acp-21-13713-2021, 2021.

Stelson, A. W. and Seinfeld, J. H.: Chemical Mass Accounting of Urban Aerosol, Environ. Sci. Technol., 15, 671–679, https://doi.org/10.1021/es00088a005, 1981.

Su, H., Cheng, Y., and Pöschl, U.: New Multiphase Chemical Processes Influencing Atmospheric Aerosols, Air Quality, and Climate in the Anthropocene, Accounts Chem. Res., 53, 2034–2043, https://doi.org/10.1021/acs.accounts.0c00246, 2020.

Sullivan, R. C., Guazzotti, S. A., Sodeman, D. A., and Prather, K. A.: Direct observations of the atmospheric processing of Asian mineral dust, Atmos. Chem. Phys., 7, 1213–1236, https://doi.org/10.5194/acp-7-1213-2007, 2007.

Tang, M., Cziczo, D. J., and Grassian, V. H.: Interactions of water with mineral dust aerosol: water adsorption, hygroscopicity, cloud condensation, and ice nucleation, Chem. Rev., 116, 4205–4259, https://doi.org/10.1021/acs.chemrev.5b00529, 2016.

Tang, M., Huang, X., Lu, K., Ge, M., Li, Y., Cheng, P., Zhu, T., Ding, A., Zhang, Y., Gligorovski, S., Song, W., Ding, X., Bi, X., and Wang, X.: Heterogeneous reactions of mineral dust aerosol: implications for tropospheric oxidation capacity, Atmos. Chem. Phys., 17, 11727–11777, https://doi.org/10.5194/acp-17-11727-2017, 2017.

Tang, M., Zhang, H., Gu, W., Gao, J., Jian, X., Shi, G., Zhu, B., Xie, L., Guo, L., Gao, X., Wang, Z., Zhang, G., and Wang, X.: Hygroscopic Properties of Saline Mineral Dust From Different Regions in China: Geographical Variations, Compositional Dependence, and Atmospheric Implications, J. Geophys. Res.-Atmos., 124, 10844–10857, https://doi.org/10.1029/2019JD031128, 2019.

Tao, W., Su, H., Zheng, G., Wang, J., Wei, C., Liu, L., Ma, N., Li, M., Zhang, Q., Pöschl, U., and Cheng, Y.: Aerosol pH and chemical regimes of sulfate formation in aerosol water during winter haze in the North China Plain, Atmos. Chem. Phys., 20, 11729–11746, https://doi.org/10.5194/acp-20-11729-2020, 2020.

Textor, C., Schulz, M., Guibert, S., Kinne, S., Balkanski, Y., Bauer, S., Berntsen, T., Berglen, T., Boucher, O., Chin, M., Dentener, F., Diehl, T., Easter, R., Feichter, H., Fillmore, D., Ghan, S., Ginoux, P., Gong, S., Grini, A., Hendricks, J., Horowitz, L., Huang, P., Isaksen, I., Iversen, T., Kloster, S., Koch, D., A. Kirkevag, Kristjansson, J. E., Krol, M., Lauer, A., Lamarque, J. F., Liu, X., Montanaro, V., Myhre, G., Penner, J., Pitari, G., Reddy, S., Seland, Ø., Stier, P., Takemura, T., and Tie, X.: Analysis and quantification of the diversities of aerosol life cycles within AeroCom, Atmos. Chem. Phys., 6, 1777–1813, https://doi.org/10.5194/acp-6-1777-2006, 2006.

Tian, R., Ma, X., Sha, T., Pan, X., and Wang, Z.: Exploring dust heterogeneous chemistry over China: Insights from field observation and GEOS-Chem simulation, Sci. Total Environ., 798, 149307, https://doi.org/10.1016/j.scitotenv.2021.149307, 2021.

Tilgner, A., Schaefer, T., Alexander, B., Barth, M., Collett Jr., J. L., Fahey, K. M., Nenes, A., Pye, H. O. T., Herrmann, H., and McNeill, V. F.: Acidity and the multiphase chemistry of atmospheric aqueous particles and clouds, Atmos. Chem. Phys., 21, 13483–13536, https://doi.org/10.5194/acp-21-13483-2021, 2021.

Tutsak, E. and Koçak, M.: High time-resolved measurements of water-soluble sulfate, nitrate and ammonium in $PM_{2.5}$ and their precursor gases over the Eastern Mediterranean, Sci. Total Environ., 672, 212–226, https://doi.org/10.1016/j.scitotenv.2019.03.451, 2019.

Ullerstam, M., Vogt, R., Langer, S., and Ljungström, E.: The kinetics and mechanism of SO_2 oxidation by O_3 on mineral dust, Phys. Chem. Chem. Phys., 4, 4694–4699, https://doi.org/10.1039/B203529B, 2002.

Ullerstam, M., Johnson, M. S., Vogt, R., and Ljungstrom, E.: DRIFTS and Knudsen cell study of the heterogeneous reactivity of SO_2 and NO_2 on mineral dust, Atmos. Chem. Phys., 3, 2043–2051, https://doi.org/10.5194/acp-3-2043-2003, 2003.

Uno, I., Eguchi, K., Yumimoto, K., Takemura, T., Shimizu, A., Uematsu, M., Liu, Z., Wang, Z., Hara, Y., and Sugimoto, N.: Asian dust transported one full circuit around the globe, Nat. Geosci., 2, 557–560, https://doi.org/10.1038/ngeo583, 2009.

Urupina, D., Lasne, J., Romanias, M. N., Thiery, V., Dagsson-Waldhauserova, P., and Thevenet, F.: Uptake and surface chemistry of SO_2 on natural volcanic dusts, Atmos. Environ., 217, 116942, https://doi.org/10.1016/j.atmosenv.2019.116942, 2019.

Urupina, D., Gaudion, V., Romanias, M. N., Verriele, M., and Thevenet, F.: Method development and validation for the determination of sulfites and sulfates on the surface of mineral atmospheric samples using reverse-phase liquid chromatography, Talanta, 219, 121318, https://doi.org/10.1016/j.talanta.2020.121318, 2020.

Urupina, D., Romanias, M. N., and Thevenet, F.: How Relevant Is It to Use Mineral Proxies to Mimic the Atmospheric Reactivity of Natural Dust Samples? A Reactivity Study Using SO_2 as Probe Molecule, Minerals, 11, 282, https://doi.org/10.3390/min11030282, 2021.

Urupina, D., Gaudion, V., Romanias, M. N., and Thevenet, F.: Surface Distribution of Sulfites and Sulfates on Natural Volcanic and Desert Dusts: Impact of Humidity and Chemical Composition, ACS Earth Space Chem., 6, 642–655, https://doi.org/10.1021/acsearthspacechem.1c00321, 2022.

Usher, C. R., Al-Hosney, H., Carlos-Cuellar, S., and Grassian, V. H.: A laboratory study of the heterogeneous uptake and oxidation of sulfur dioxide on mineral dust particles, J. Geophys. Res.-Atmos., 107, 4713, https://doi.org/10.1029/2002JD002051, 2002.

Usher, C. R., Michel, A. E., and Grassian, V. H.: Reactions on mineral dust, Chem. Rev., 103, 4883–4940, https://doi.org/10.1021/cr020657y, 2003.

Volkamer, R., San Martini, F., Molina, L. T., Salcedo, D., Jimenez, J. L., and Molina, M. J.: A missing sink for gas-phase glyoxal in Mexico City: Formation of secondary organic aerosol, Geophys. Res. Lett., 34, L19807, https://doi.org/10.1029/2007GL030752, 2007.

Wang, G., Zhang, R., Gomez, M. E., Yang, L., Levy Zamora, M., Hu, M., Lin, Y., Peng, J., Guo, S., Meng, J., Li, J., Cheng, C., Hu, T., Ren, Y., Wang, Y., Gao, J., Cao, J., An, Z., Zhou, W., Li, G., Wang, J., Tian, P., Marrero-Ortiz, W., Secrest, J., Du, Z., Zheng, J., Shang, D., Zeng, L., Shao, M., Wang, W., Huang, Y., Wang, Y., Zhu, Y., Li, Y., Hu, J., Pan, B., Cai, L., Cheng, Y., Ji, Y., Zhang, F., Rosenfeld, D., Liss, P. S., Duce, R. A., Kolb, C. E., and Molina, M. J.: Persistent sulfate formation from London Fog to Chinese haze, P. Natl. Acad. Sci. USA, 113, 13630–13635, https://doi.org/10.1073/pnas.1616540113, 2016.

Wang, H., Zhong, C., Ma, Q., Ma, J., and He, H.: The adsorption and oxidation of SO_2 on MgO surface: experimental and DFT calculation studies, Environ. Sci. Nano, 7, 1092–1101, https://doi.org/10.1039/C9EN01474H, 2020.

Wang, K., Zhang, Y., Nenes, A., and Fountoukis, C.: Implementation of dust emission and chemistry into the Community Multiscale Air Quality modeling system and initial application to an Asian dust storm episode, Atmos. Chem. Phys., 12, 10209–10237, https://doi.org/10.5194/acp-12-10209-2012, 2012.

Wang, K., Hattori, S., Lin, M., Ishino, S., Alexander, B., Kamezaki, K., Yoshida, N., and Kang, S.: Isotopic constraints on atmospheric sulfate formation pathways in the Mt. Everest region, southern Tibetan Plateau, Atmos. Chem. Phys., 21, 8357–8376, https://doi.org/10.5194/acp-21-8357-2021, 2021.

Wang, R., Yang, N., Li, J., Xu, L., Tsona, N. T., Du, L., and Wang, W.: Heterogeneous reaction of SO_2 on $CaCO_3$ particles: Different impacts of NO_2 and acetic acid on the sulfite and sulfate formation, J. Environ. Sci., 114, 149–159, https://doi.org/10.1016/j.jes.2021.08.017, 2022.

Wang, S., Wang, L., Fan, X., Wang, N., Ma, S., and Zhang, R.: Formation pathway of secondary inorganic aerosol and its influencing factors in Northern China: Comparison between urban and rural sites, Sci. Total Environ., 840, 156404, https://doi.org/10.1016/j.scitotenv.2022.156404, 2022.

Wang, T.: Date for "Significant formation of sulfate aerosols contributed by the heterogeneous drivers of dust surface", Mendeley Data [data set], https://doi.org/10.17632/hyvdz7khs6.1, 2022.

Wang, T., Liu, Y., Deng, Y., Fu, H., Zhang, L., and Chen, J.: The influence of temperature on the heterogeneous uptake of SO_2 on hematite particles, Sci. Total Environ., 644, 1493–1502, https://doi.org/10.1016/j.scitotenv.2018.07.046, 2018a.

Wang, T., Liu, Y., Deng, Y., Fu, H., Zhang, L., and Chen, J.: Emerging investigator series: heterogeneous reactions of sul-

fur dioxide on mineral dust nanoparticles: from single component to mixed components, Environ. Sci. Nano, 5, 1821–1833, https://doi.org/10.1039/C8EN00376A, 2018b.

Wang, T., Liu, Y., Deng, Y., Fu, H., Zhang, L., and Chen, J.: Adsorption of SO_2 on mineral dust particles influenced by atmospheric moisture, Atmos. Environ., 191, 153–161, https://doi.org/10.1016/j.atmosenv.2018.08.008, 2018c.

Wang, T., Liu, Y., Deng, Y., Cheng, H., Fang, X., and Zhang, L.: Heterogeneous Formation of Sulfur Species on Manganese Oxides: Effects of Particle Type and Moisture Condition, J. Phys. Chem. A, 124, 7300–7312, https://doi.org/10.1021/acs.jpca.0c04483, 2020a.

Wang, T., Liu, Y., Deng, Y., Cheng, H., Yang, Y., Feng, Y., Zhang, L., Fu, H., and Chen, J.: Photochemical Oxidation of Water-Soluble Organic Carbon (WSOC) on Mineral Dust and Enhanced Organic Ammonium Formation, Environ. Sci. Technol., 54, 15631–15642, https://doi.org/10.1021/acs.est.0c04616, 2020b.

Wang, T., Liu, M., Liu, M., Song, Y., Xu, Z., Shang, F., Huang, X., Liao, W., Wang, W., Ge, M., Cao, J., Hu, J., Tang, G., Pan, Y., Hu, M., and Zhu, T.: Sulfate Formation Apportionment during Winter Haze Events in North China, Environ. Sci. Technol., 56, 7771–7778, https://doi.org/10.1021/acs.est.2c02533, 2022.

Wang, W., Liu, M., Wang, T., Song, Y., Zhou, L., Cao, J., Hu, J., Tang, G., Chen, Z., Li, Z., Xu, Z., Peng, C., Lian, C., Chen, Y., Pan, Y., Zhang, Y., Sun, Y., Li, W., Zhu, T., Tian, H., and Ge, M.: Sulfate formation is dominated by manganese-catalyzed oxidation of SO_2 on aerosol surfaces during haze events, Nat. Commun., 12, 1993, https://doi.org/10.1038/s41467-021-22091-6, 2021.

Wang, X., Gemayel, R., Hayeck, N., Perrier, S., Charbonnel, N., Xu, C., Chen, H., Zhu, C., Zhang, L., Wang, L., Nizkorodov, S. A., Wang, X., Wang, Z., Wang, T., Mellouki, A., Riva, M., Chen, J., and George, C.: Atmospheric Photosensitization: A New Pathway for Sulfate Formation, Environ. Sci. Technol., 54, 3114–3120, https://doi.org/10.1021/acs.est.9b06347, 2020.

Wang, Y., Zhang, Q., Jiang, J., Zhou, W., Wang, B., He, K., Duan, F., Zhang, Q., Philip, S., and Xie, Y.: Enhanced sulfate formation during China's severe winter haze episode in January 2013 missing from current models, J. Geophys. Res., 119, 10425–10440, https://doi.org/10.1002/2013jd021426, 2014.

Wang, Z., Wang, T., Fu, H., Zhang, L., Tang, M., George, C., Grassian, V. H., and Chen, J.: Enhanced heterogeneous uptake of sulfur dioxide on mineral particles through modification of iron speciation during simulated cloud processing, Atmos. Chem. Phys., 19, 12569–12585, https://doi.org/10.5194/acp-19-12569-2019, 2019.

Wu, C., Zhang, S., Wang, G., Lv, S., Li, D., Liu, L., Li, J., Liu, S., Du, W., Meng, J., Qiao, L., Zhou, M., Huang, C., and Wang, H.: Efficient Heterogeneous Formation of Ammonium Nitrate on the Saline Mineral Particle Surface in the Atmosphere of East Asia during Dust Storm Periods, Environ. Sci. Technol., 54, 15622–15630, https://doi.org/10.1021/acs.est.0c04544, 2020.

Wu, L., Tong, S., Zhou, L., Wang, W., and Ge, M.: Synergistic effects between SO_2 and HCOOH on α-Fe_2O_3, J. Phys. Chem. A, 117, 3972–3979, https://doi.org/10.1021/jp400195f, 2013.

Wu, L. Y., Tong, S. R., Wang, W. G., and Ge, M. F.: Effects of temperature on the heterogeneous oxidation of sulfur dioxide by ozone on calcium carbonate, Atmos. Chem. Phys., 11, 6593–6605, https://doi.org/10.5194/acp-11-6593-2011, 2011.

Wu, Z., Wang, Y., Tan, T., Zhu, Y., Li, M., Shang, D., Wang, H., Lu, K., Guo, S., Zeng, L., and Zhang, Y.: Aerosol Liquid Water Driven by Anthropogenic Inorganic Salts: Implying Its Key Role in Haze Formation over the North China Plain, Environ. Sci. Technol. Lett., 5, 160–166, https://doi.org/10.1021/acs.estlett.8b00021, 2018.

Xu, M., Qiu, P., He, Y., Guo, S., Bai, Y., Zhang, H., Zhao, S., Shen, X., Zhu, B., Guo, Q., and Guo, Z.: Sulfur isotope composition during heterogeneous oxidation of SO_2 on mineral dust: The effect of temperature, relative humidity, and light intensity, Atmos. Res., 254, 105513, https://doi.org/10.1016/j.atmosres.2021.105513, 2021.

Xu, W., Kuang, Y., Liang, L., He, Y., Cheng, H., Bian, Y., Tao, J., Zhang, G., Zhao, P., Ma, N., Zhao, H., Zhou, G., Su, H., Cheng, Y., Xu, X., Shao, M., and Sun, Y.: Dust-Dominated Coarse Particles as a Medium for Rapid Secondary Organic and Inorganic Aerosol Formation in Highly Polluted Air, Environ. Sci. Technol., 54, 15710–15721, https://doi.org/10.1021/acs.est.0c07243, 2020.

Xue, J., Yuan, Z., Griffith, S. M., Yu, X., Lau, A. K. H., and Yu, J. Z.: Sulfate formation enhanced by a cocktail of high NO_x, SO_2, particulate matter, and droplet pH during haze-fog events in megacities in China: an observation-based modeling investigation, Environ. Sci. Technol., 50, 7325–7334, https://doi.org/10.1021/acs.est.6b00768, 2016.

Yang, L., Yu, L. E., and Ray, M. B.: Degradation of paracetamol in aqueous solutions by TiO_2 photocatalysis, Water Res., 42, 3480–3488, https://doi.org/10.1016/j.watres.2008.04.023, 2008.

Yang, N., Tsona, N. T., Cheng, S., Li, S., Xu, L., Wang, Y., Wu, L., and Du, L.: Competitive reactions of SO_2 and acetic acid on α-Al_2O_3 and $CaCO_3$ particles, Sci. Total Environ., 699, 134362, https://doi.org/10.1016/j.scitotenv.2019.134362, 2020.

Yang, W., He, H., Ma, Q., Ma, J., Liu, Y., Liu, P., and Mu, Y.: Synergistic formation of sulfate and ammonium resulting from reaction between SO_2 and NH_3 on typical mineral dust, Phys. Chem. Chem. Phys., 18, 956–964, https://doi.org/10.1039/C5CP06144J, 2016.

Yang, W., Zhang, J., Ma, Q., Zhao, Y., Liu, Y., and He, H.: Heterogeneous reaction of SO_2 on manganese oxides: the effect of crystal structure and relative humidity, Sci. Rep.-UK, 7, 4550, https://doi.org/10.1038/s41598-017-04551-6, 2017.

Yang, W., Chen, M., Xiao, W., Guo, Y., Ding, J., Zhang, L., and He, H.: Molecular Insights into NO-Promoted Sulfate Formation on Model TiO_2 Nanoparticles with Different Exposed Facets, Environ. Sci. Technol., 52, 14110–14118, https://doi.org/10.1021/acs.est.8b02688, 2018a.

Yang, W., Ma, Q., Liu, Y., Ma, J., Chu, B., Wang, L., and He, H.: Role of NH_3 in the Heterogeneous Formation of Secondary Inorganic Aerosols on Mineral Oxides, J. Phys. Chem. A, 122, 6311–6320, https://doi.org/10.1021/acs.jpca.8b05130, 2018b.

Yang, W., Ma, Q., Liu, Y., Ma, J., Chu, B., and He, H.: The effect of water on the heterogeneous reactions of SO_2 and NH_3 on the surfaces of α-Fe_2O_3 and γ-Al_2O_3, Environ. Sci. Nano, 6, 2749–2758, https://doi.org/10.1039/C9EN00574A, 2019.

Ye, C., Liu, P., Ma, Z., Xue, C., Zhang, C., Zhang, Y., Liu, J., Liu, C., Sun, X., and Mu, Y.: High H_2O_2 Concentrations Observed during Haze Periods during the Winter in Beijing: Importance

of H_2O_2 Oxidation in Sulfate Formation, Environ. Sci. Technol. Lett., 5, 757–763, https://doi.org/10.1021/acs.estlett.8b00579, 2018.

Ye, C., Lu, K., Song, H., Mu, Y., Chen, J., and Zhang, Y.: A critical review of sulfate aerosol formation mechanisms during winter polluted periods, J. Environ. Sci., in press, https://doi.org/10.1016/j.jes.2022.07.011, 2022.

Yin, Z., Wan, Y., Zhang, Y., and Wang, H.: Why super sandstorm 2021 in North China, Natl. Sci. Rev., 9, nwab165, https://doi.org/10.1093/nsr/nwab165, 2021.

Yu, J.: An interfacial role for NO_2, Nat. Chem., 13, 1158–1160, https://doi.org/10.1038/s41557-021-00845-5, 2021.

Yu, T., Zhao, D., Song, X., and Zhu, T.: NO_2-initiated multiphase oxidation of SO_2 by O_2 on $CaCO_3$ particles, Atmos. Chem. Phys., 18, 6679–6689, https://doi.org/10.5194/acp-18-6679-2018, 2018.

Yu, Z., Jang, M., and Park, J.: Modeling atmospheric mineral aerosol chemistry to predict heterogeneous photooxidation of SO_2, Atmos. Chem. Phys., 17, 10001–10017, https://doi.org/10.5194/acp-17-10001-2017, 2017.

Yue, F., Xie, Z., Zhang, P., Song, S., He, P., Liu, C., Wang, L., Yu, X., and Kang, H.: The role of sulfate and its corresponding $S_{(IV)} + NO_2$ formation pathway during the evolution of haze in Beijing, Sci. Total Environ., 687, 741–751, https://doi.org/10.1016/j.scitotenv.2019.06.096, 2019.

Zhang, F., Wang, Y., Peng, J., Chen, L., Sun, Y., Duan, L., Ge, X., Li, Y., Zhao, J., Liu, C., Zhang, X., Zhang, G., Pan, Y., Wang, Y., Zhang, A. L., Ji, Y., Wang, G., Hu, M., Molina, M. J., and Zhang, R.: An unexpected catalyst dominates formation and radiative forcing of regional haze, P. Natl. Acad. Sci. USA, 117, 3960–3966, https://doi.org/10.1073/pnas.1919343117, 2020.

Zhang, H., Xu, Y., and Jia, L.: A chamber study of catalytic oxidation of SO_2 by Mn^{2+} / Fe^{3+} in aerosol water, Atmos. Environ., 245, 118019, https://doi.org/10.1016/j.atmosenv.2020.118019, 2021.

Zhang, R., Wang, G., Guo, S., Zamora, M. L., Ying, Q., Lin, Y., Wang, W., Hu, M., and Wang, Y.: Formation of urban fine particulate matter, Chem. Rev., 115, 3803–3855, https://doi.org/10.1021/acs.chemrev.5b00067, 2015.

Zhang, S., Xing, J., Sarwar, G., Ge, Y., He, H., Duan, F., Zhao, Y., He, K., Zhu, L., and Chu, B.: Parameterization of heterogeneous reaction of SO_2 to sulfate on dust with coexistence of NH_3 and NO_2 under different humidity conditions, Atmos. Environ., 208, 133–140, https://doi.org/10.1016/j.atmosenv.2019.04.004, 2019.

Zhang, X., Zhuang, G., Chen, J., Wang, Y., Wang, X., An, Z., and Zhang, P.: Heterogeneous reaction of sulfur dioxide on typical mineral particles, J. Phys. Chem. B, 110, 12588–12596, https://doi.org/10.1021/jp0617773, 2006.

Zhang, X. Y., Wang, Y. Q., Niu, T., Zhang, X. C., Gong, S. L., Zhang, Y. M., and Sun, J. Y.: Atmospheric aerosol compositions in China: spatial/temporal variability, chemical signature, regional haze distribution and comparisons with global aerosols, Atmos. Chem. Phys., 12, 779–799, https://doi.org/10.5194/acp-12-779-2012, 2012.

Zhang, Y., Tong, S. R., and Ge, M. F.: A study about the influence of the size of $CaCO_3$ on the heterogeneous oxidation of sulfur dioxide by ozone, Spectrosc. Spect. Anal., 36, 126–127, 2016.

Zhang, Y., Tong, S., Ge, M., Jing, B., Hou, S., Tan, F., Chen, Y., Guo, Y., and Wu, L.: The influence of relative humidity on the heterogeneous oxidation of sulfur dioxide by ozone on calcium carbonate particles, Sci. Total Environ., 633, 1253–1262, https://doi.org/10.1016/j.scitotenv.2018.03.288, 2018.

Zhang, Y., Bao, F., Li, M., Chen, C., and Zhao, J.: Nitrate-Enhanced Oxidation of SO_2 on Mineral Dust: A Vital Role of a Proton, Environ. Sci. Technol., 53, 10139–10145, https://doi.org/10.1021/acs.est.9b01921, 2019.

Zhanzakova, A., Tong, S., Yang, K., Chen, L., Li, K., Fu, H., Wang, L., and Kong, L.: The effects of surfactants on the heterogeneous uptake of sulfur dioxide on hematite, Atmos. Environ., 213, 548–557, https://doi.org/10.1016/j.atmosenv.2019.06.050, 2019.

Zhao, D., Song, X., Zhu, T., Zhang, Z., Liu, Y., and Shang, J.: Multiphase oxidation of SO_2 by NO_2 on $CaCO_3$ particles, Atmos. Chem. Phys., 18, 2481–2493, https://doi.org/10.5194/acp-18-2481-2018, 2018.

Zhao, X., Kong, L., Sun, Z., Ding, X., Cheng, T., Yang, X., and Chen, J.: Interactions between heterogeneous uptake and adsorption of sulfur dioxide and acetaldehyde on hematite, J. Phys. Chem. A, 119, 4001–4008, https://doi.org/10.1021/acs.jpca.5b01359, 2015.

Zheng, B., Zhang, Q., Zhang, Y., He, K. B., Wang, K., Zheng, G. J., Duan, F. K., Ma, Y. L., and Kimoto, T.: Heterogeneous chemistry: a mechanism missing in current models to explain secondary inorganic aerosol formation during the January 2013 haze episode in North China, Atmos. Chem. Phys., 15, 2031–2049, https://doi.org/10.5194/acp-15-2031-2015, 2015.

Zheng, H., Song, S., Sarwar, G., Gen, M., Wang, S., Ding, D., Chang, X., Zhang, S., Xing, J., Sun, Y., Ji, D., Chan, C. K., Gao, J., and McElroy, M. B.: Contribution of Particulate Nitrate Photolysis to Heterogeneous Sulfate Formation for Winter Haze in China, Environ. Sci. Technol. Lett., 7, 632–638, https://doi.org/10.1021/acs.estlett.0c00368, 2020.

Zheng, S., Huang, Q., Zhou, J., and Wang, B.: A study on dye photoremoval in TiO_2 suspension solution, J. Photochem. Photobiol., A, 108, 235–238, https://doi.org/10.1016/S1010-6030(97)00014-2, 1997.

Zhou, L., Wang, W., Gai, Y., and Ge, M.: Knudsen cell and smog chamber study of the heterogeneous uptake of sulfur dioxide on Chinese mineral dust, J. Environ. Sci., 26, 2423–2433, https://doi.org/10.1016/j.jes.2014.04.005, 2014.

Zhu, Y., Toon, O. B., Jensen, E. J., Bardeen, C. G., Mills, M. J., Tolbert, M. A., Yu, P., and Woods, S.: Persisting volcanic ash particles impact stratospheric SO_2 lifetime and aerosol optical properties, Nat. Commun., 11, 4526, https://doi.org/10.1038/s41467-020-18352-5, 2020.